

Effective Lagrangian description of top quark production and decay

G. J. Gounaris

Department of Theoretical Physics, University of Thessaloniki, Gr-54006, Thessaloniki, Greece

M. Kuroda

Institute of Physics, Meiji-Gakuin University, Yokohama, Japan

F. M. Renard

Physique Mathématique et Théorique, UPRES-A 5032, Université Montpellier II, F-34095 Montpellier Cedex 5, France

(Received 26 June 1996)

We propose a rather general description of residual new physics (NP) effects on the top quark couplings. These effects are described in terms of 20 gauge-invariant $\text{dim}=6$ operators involving gauge and Higgs bosons as well as quarks of the third family. We compute their implications for the $\gamma t\bar{t}$, $Z t\bar{t}$, and $t b W$ vertices and study their observability in the process $e^- e^+ \rightarrow t\bar{t}$ with $t \rightarrow b W \rightarrow b \ell^+ \nu_\ell$. We present results for the integrated cross section, the angular distribution, and various decay distribution and polarization asymmetries for NLC energies of 0.5–2 TeV. Observability limits are discussed and interpreted in terms of the NP scales associated with each operator through the unitarity constraints. The general landscape of the residual NP effects in the heavy quark and bosonic sectors is also presented. [S0556-2821(96)03623-5]

PACS number(s): 14.65.Ha, 12.15.Ji, 13.38.Dg, 14.70.Hp

I. INTRODUCTION

It is commonly hoped that the high value of the top quark mass may open a window towards understanding the mass generation mechanism. It is then important to look at the top quark interactions in a very accurate way, searching for possible departures from universality, which are somehow associated with the heavy t mass, i.e., differences from the properties of the light quarks and leptons. This is particularly true if no new particles are lying within the reach of the contemplated colliders. Such top-quark-mass effects are of course well known for certain standard model (SM) electroweak radiative corrections. They increase like m_t^2 , as, e.g., in the so-called $\delta\rho$ or ϵ_1 parameters [1]. Our search for new physics (NP) will then concentrate on whether there exist any additional effects, somehow related to the scalar sector and the large top-quark-mass m_t , which are beyond those expected in the SM.

The most intriguing hint towards this kind of NP is provided by the present situation concerning the $Z b\bar{b}$ vertex. This vertex receives a well-known SM contribution [2] proportional to m_t^2 , which does not seem sufficient though, to explain the data. Indeed, the experimental results at the CERN $e^+ e^-$ collider LEP 1 and at the SLAC Linear Collider (SLC) suggest that the SM top quark effect in ϵ_1 agrees with the top quark mass value found at Fermilab, while no corresponding agreement is observed for $\Gamma(Z \rightarrow b\bar{b})$ [3]. Thus, if the present experimental result on $\Gamma(Z \rightarrow b\bar{b})$ is correct, it probably indicates the appearance of a mechanism whose origin must lie beyond the SM. Various types of ideas for this new physics are possible, partially stemming from the fact that the left-versus-right structure of the $Z b\bar{b}$ vertex is not yet completely established [4–6].

An additional measurement allowing one to determine the asymmetry factor A_b is required to clarify the $Z \rightarrow b\bar{b}$ situa-

tion. This can be achieved either by measuring the forward-backward asymmetry at LEP 1 or, more directly, from the measurement at SLC of the polarized forward-backward asymmetry [3]. At present there exists some disagreement between these two measurements. But in any case, the data seem to suggest that if a NP effect is present, then it should predominantly be affecting the right-handed $Z b\bar{b}$ amplitude. The situation is further complicated by the observation of a (weaker) anomalous effect in the $Z c\bar{c}$ vertex, which cannot be associated with an obvious virtual top quark contribution and requires a more direct NP source affecting light quarks also [7].

We assume here that in the foreseeable future no new particles will be found, beyond those present in¹ SM. In such a case, NP could only appear in the form of residual interactions generated at a very large scale, i.e., $\Lambda_{NP} \gg M_W$. It may turn out that these residual interactions stem from the scalar sector and affect only the Higgs boson and its “partners,” i.e., the fermions coupled most strongly to the scalar sector and the gauge bosons. Under these conditions, NP should be described by an effective Lagrangian expressed in terms of $\text{SU}(3)_c \times \text{SU}(2) \times \text{U}(1)$ gauge-invariant $\text{dim}=6$ operators, involving the Higgs boson together with W , Z , γ , the quarks of the third family, and the gluon. To somewhat restrict the number of such operators, we impose the constraint that the quark-dependent operators should necessarily involve at least one t_R field [5]. We do this motivated by the form of the SM Yukawa couplings in the limit where all fermion masses, except the top quark, are neglected. In the present work we also impose CP invariance for NP, and disregard operators which (after the use of the equations of motion) would have rendered four-quark operators involving leptons or light quarks of the first two families.

¹The Higgs boson is an old particle in this sense.

There exist 14 such CP -conserving ‘‘top’’ operators which have been classified in [5]. In addition, there exist 6 CP -conserving purely bosonic ones, which are ‘‘blind’’ with respect to LEP 1 physics and have been studied in [8,9]. The indirect constraints on these operators from the LEP 1 and SLC measurements (including those from $Z \rightarrow b\bar{b}$) have been established in [5] for the ‘‘top’’ operators and in [9,8,4] for the bosonic ones. These constraints appear to be quite mild, calling for a more detailed study in a higher energy collider. Towards this aim, the observable signatures of the bosonic NP operators through the high energy processes $e^+e^- \rightarrow W^+W^-$ [10,11], $e^+e^- \rightarrow HZ$, and $e^+e^- \rightarrow H\gamma$ [12,13] have already been studied.

In the present work we are interested in the more *direct tests* of the above operators that will be provided by the real top quark production process $e^+e^- \rightarrow t\bar{t}$ and the decay $t \rightarrow Wb \rightarrow bl^+\nu$. Such a study should considerably improve the existing sensitivity limits on this kind of NP. Since we expect the NP effects to be rather small, it is sufficient for the calculation to restrict ourselves to the leading contributions. Thus, we either restrict ourselves to the tree-level contribution, whenever this is nonvanishing or (if it vanishes) retain only the leading-logarithmic one-loop effect, provided it is enhanced by a power of the large top quark mass m_t . Under these conditions, box diagrams are never important in our studies. Thus, we just need to determine the NP effects on the $\gamma t\bar{t}$, $Zt\bar{t}$, and tbW vertices.

The interesting physical quantities are the integrated cross section, the density matrix of the produced t quark, and various angular distributions. We show how the density matrix elements can be measured through decay distributions with or without e^\pm -beam polarization. The sensitivities of the various observables to each operator are presented and the observability limits for the associated couplings are established. With the help of unitarity relations, these limits are translated into lower bounds on the scale of corresponding new physics. Finally we draw the panorama of the knowledge that one can reach on the whole set of top and bosonic operators through these tests, as well as through the previous indirect ones.

The paper is organized as follows. In Sec. II we enumerate the dim=6 operators used to construct the effective NP Lagrangian, and define their couplings and associated NP scales. In Sec. III we compute the corresponding general $e^+e^- \rightarrow t\bar{t}$ helicity amplitude and the top quark density matrix. Section IV is devoted to the $t \rightarrow bW \rightarrow b\ell^+\nu_\ell$ decay of the produced top quark. In Sec. V we compute the SM one-loop m_t^2 -enhanced contributions to these amplitudes, and in Sec. VI the leading NP contributions for all operators are considered. The resulting panorama of residual NP effects is discussed in Sec. VII. Two appendixes give details about the computations of the NP effects and the decay distributions and asymmetries.

II. EFFECTIVE LAGRANGIAN

The list of the dim=6, $SU(3)_c \times SU(2) \times U(1)$ gauge-invariant and CP -conserving operators involving the third

family of quarks with at least one t_R field,² together with gauge and scalar boson fields, has been established in [5]. These operators are divided into two groups containing four and two quark fields, respectively.

(1) *Four-quark operators:*

$$\mathcal{O}_{qt} = (\bar{q}_L t_R)(\bar{t}_R q_L), \quad (1)$$

$$\mathcal{O}_{qt}^{(8)} = (\bar{q}_L \vec{\lambda} t_R)(\bar{t}_R \vec{\lambda} q_L), \quad (2)$$

$$\mathcal{O}_{tt} = \frac{1}{2}(\bar{t}_R \gamma_\mu t_R)(\bar{t}_R \gamma^\mu t_R), \quad (3)$$

$$\mathcal{O}_{tb} = (\bar{t}_R \gamma_\mu t_R)(\bar{b}_R \gamma^\mu b_R), \quad (4)$$

$$\mathcal{O}_{tb}^{(8)} = (\bar{t}_R \gamma_\mu \vec{\lambda} t_R)(\bar{b}_R \gamma^\mu \vec{\lambda} b_R), \quad (5)$$

$$\begin{aligned} \mathcal{O}_{qq} &= (\bar{t}_R t_L)(\bar{b}_R b_L) + (\bar{t}_L t_R)(\bar{b}_L b_R) - (\bar{t}_R b_L)(\bar{b}_R t_L) \\ &\quad - (\bar{b}_L t_R)(\bar{t}_L b_R), \end{aligned} \quad (6)$$

$$\begin{aligned} \mathcal{O}_{qq}^{(8)} &= (\bar{t}_R \vec{\lambda} t_L)(\bar{b}_R \vec{\lambda} b_L) + (\bar{t}_L \vec{\lambda} t_R)(\bar{b}_L \vec{\lambda} b_R) - (\bar{t}_R \vec{\lambda} b_L)(\bar{b}_R \vec{\lambda} t_L) \\ &\quad - (\bar{b}_L \vec{\lambda} t_R)(\bar{t}_L \vec{\lambda} b_R). \end{aligned} \quad (7)$$

(2) *Two-quark operators:*

$$\mathcal{O}_{t1} = (\Phi^\dagger \Phi)(\bar{q}_L t_R \vec{\Phi} + \bar{t}_R \vec{\Phi}^\dagger q_L), \quad (8)$$

$$\mathcal{O}_{t2} = i[\Phi^\dagger (D_\mu \Phi) - (D_\mu \Phi^\dagger) \Phi](\bar{t}_R \gamma^\mu t_R), \quad (9)$$

$$\mathcal{O}_{t3} = i(\vec{\Phi}^\dagger D_\mu \Phi)(\bar{t}_R \gamma^\mu b_R) - i(D_\mu \Phi^\dagger \vec{\Phi})(\bar{b}_R \gamma^\mu t_R), \quad (10)$$

$$\mathcal{O}_{Dt} = (\bar{q}_L D_\mu t_R) D^\mu \vec{\Phi} + D^\mu \vec{\Phi}^\dagger [(D_\mu \bar{t}_R) q_L], \quad (11)$$

$$\mathcal{O}_{tW\Phi} = (\bar{q}_L \sigma^{\mu\nu} \vec{\tau} t_R) \vec{\Phi} \cdot \vec{W}_{\mu\nu} + \vec{\Phi}^\dagger (\bar{t}_R \sigma^{\mu\nu} \vec{\tau} q_L) \cdot \vec{W}_{\mu\nu}, \quad (12)$$

$$\mathcal{O}_{tB\Phi} = (\bar{q}_L \sigma^{\mu\nu} t_R) \vec{\Phi} B_{\mu\nu} + \vec{\Phi}^\dagger (\bar{t}_R \sigma^{\mu\nu} q_L) B_{\mu\nu}, \quad (13)$$

$$\mathcal{O}_{tG\Phi} = [(\bar{q}_L \sigma^{\mu\nu} \lambda^a t_R) \vec{\Phi} + \vec{\Phi}^\dagger (\bar{t}_R \sigma^{\mu\nu} \lambda^a q_L)] G_{\mu\nu}^a, \quad (14)$$

where $\lambda^a (a=1, \dots, 8)$ are the usual eight color matrices.

In the preceding formulas the definitions

$$\Phi = \begin{pmatrix} i\chi^+ \\ \frac{1}{\sqrt{2}}(v + H - i\chi^3) \end{pmatrix}, \quad (15)$$

$$D_\mu = \left(\partial_\mu + ig' Y B_\mu + i \frac{g}{2} \vec{\tau} \cdot \vec{W}_\mu + i \frac{g_s}{2} \vec{\lambda} \cdot \vec{G}_\mu \right) \quad (16)$$

are used where $v \simeq 246$ GeV, Y is the hypercharge of the field on which the covariant derivative acts, and $\vec{\tau}$ and $\vec{\lambda}$ are the isospin and color matrices applicable whenever D_μ acts

²These quark fields are of course understood as the weak eigenstate fields. They are related to the fields creating or absorbing the mass eigenstates through the usual unitary transformations leading to the Cabibbo-Kobayashi-Maskawa (CKM) matrix.

on isodoublet fermions and quarks, respectively. As already stated, in writing Eqs. (1)–(14), we have used the equations of motion. If these latter equations were not used, then two more operators are met which contain additional derivatives [14].

(3) *Bosonic operators*: In addition to the above fermionic $\dim=6$ operators, NP may also be hiding in purely bosonic ones. Provided CP invariance is imposed, this kind of NP is described by 11 $\dim=6$ purely bosonic operators first classified in [8]. Here, we retain only the six ‘‘blind’’ or ‘‘super-blind’’ ones [15], which are not severely constrained by the Z-peak experiments [16]. They are

$$\mathcal{O}_W = \frac{1}{3!} (\vec{W}_\mu^\nu \times \vec{W}_\nu^\lambda) \cdot \vec{W}_\lambda^\mu, \quad (17)$$

$$\mathcal{O}_{W\Phi} = i(D_\mu \Phi)^\dagger \vec{\tau} \cdot \vec{W}^{\mu\nu} (D_\nu \Phi), \quad (18)$$

$$\mathcal{O}_{B\Phi} = i(D_\mu \Phi)^\dagger B^{\mu\nu} (D_\nu \Phi), \quad (19)$$

$$\mathcal{O}_{UW} \equiv \frac{1}{v^2} \left(\Phi^\dagger \Phi - \frac{v^2}{2} \right) \vec{W}^{\mu\nu} \cdot \vec{W}_{\mu\nu}, \quad (20)$$

$$\mathcal{O}_{UB} \equiv \frac{4}{v^2} \left(\Phi^\dagger \Phi - \frac{v^2}{2} \right) B^{\mu\nu} B_{\mu\nu}, \quad (21)$$

$$\mathcal{O}_{\Phi 2} = 4 \partial_\mu (\Phi^\dagger \Phi) \partial^\mu (\Phi^\dagger \Phi). \quad (22)$$

The remaining five operators (called $\mathcal{O}_{DW}, \mathcal{O}_{DB}, \mathcal{O}_{BW}, \mathcal{O}_{\Phi 1}$, and $\mathcal{O}_{\Phi 3}$) [8] are ignored here, since they are either too severely constrained or they give no contribution (up to the one-loop level) to the processes we study.³

The resulting effective Lagrangian describing the residual NP interactions is written as

$$\mathcal{L} = \mathcal{L}_t + \mathcal{L}_{\text{bos}}, \quad (23)$$

where the contribution from the 14 ($i=1, \dots, 14$) ‘‘top’’ operators is

$$\mathcal{L}_t = \sum_i \frac{f_i}{m_i^2} \mathcal{O}_i, \quad (24)$$

while the purely bosonic ones give

$$\begin{aligned} \mathcal{L}_{\text{bos}} = & \lambda_W \frac{g}{M_W^2} \mathcal{O}_W + f_W \frac{g}{2M_W^2} \mathcal{O}_{W\Phi} + f_B \frac{g'}{2M_W^2} \mathcal{O}_{B\Phi} + d \mathcal{O}_{UW} \\ & + \frac{d_B}{4} \mathcal{O}_{UB} + \frac{f_{\Phi 2}}{v^2} \mathcal{O}_{\Phi 2}. \end{aligned} \quad (25)$$

As a whole we have 20 independent operators that we shall occasionally globally label as \mathcal{O}_i , with $i=1, \dots, 20$.

To each of the coupling constants f_i (or λ_W, d, d_B) appearing in this Lagrangian, a corresponding new physics scale Λ_{NP} is associated through the unitarity relations established in [18,12,14]. Obviously Λ_{NP} generally depends on

the operator \mathcal{O}_i considered. Thus for the purely bosonic operators we have found [18,12]

$$|\lambda_W| \simeq 19 \frac{M_W^2}{\Lambda_{\text{NP}}^2}, \quad |f_B| \simeq 98 \frac{M_W^2}{\Lambda_{\text{NP}}^2}, \quad |f_W| \simeq 31 \frac{M_W^2}{\Lambda_{\text{NP}}^2}, \quad (26)$$

$$d \simeq \frac{104.5(M_W/\Lambda_{\text{NP}})^2}{1+6.5(M_W/\Lambda_{\text{NP}})} \text{ for } d > 0,$$

$$d \simeq -\frac{104.5(M_W/\Lambda_{\text{NP}})^2}{1-4(M_W/\Lambda_{\text{NP}})} \text{ for } d < 0, \quad (27)$$

$$d_B \simeq \frac{195.8(M_W/\Lambda_{\text{NP}})^2}{1+200(M_W/\Lambda_{\text{NP}})^2} \text{ for } d_B > 0,$$

$$d_B \simeq -\frac{195.8(M_W/\Lambda_{\text{NP}})^2}{1+50(M_W/\Lambda_{\text{NP}})^2} \text{ for } d_B < 0, \quad (28)$$

while for $\mathcal{O}_{\Phi 2}$ and $\Lambda_{\text{NP}} \sim 3.7$ TeV we have no constraint for $f_{\Phi 2} > 0$, and

$$f_{\Phi 2} \simeq \frac{-16 - a_w + \sqrt{a_w(a_w + 32)}}{128} \text{ for } f_{\Phi 2} < 0, \quad (29)$$

where $a_w = \alpha \sqrt{3} \Lambda_{\text{NP}}^2 / (4s_W^2 M_W^2)$ [12].

On the other hand, for the 14 ‘‘top’’ operators, unitarity gives⁴ [14]

$$|f_{qt}| \simeq \frac{16\pi}{3} \left(\frac{m_t^2}{\Lambda_{\text{NP}}^2} \right), \quad (30)$$

$$|f_{qt}^{(8)}| \simeq \frac{9\pi}{\sqrt{2}} \left(\frac{m_t^2}{\Lambda_{\text{NP}}^2} \right), \quad (31)$$

$$|f_{tt}| \simeq 6\pi \left(\frac{m_t^2}{\Lambda_{\text{NP}}^2} \right), \quad (32)$$

$$|f_{tb}| \simeq 8\pi \left(\frac{m_t^2}{\Lambda_{\text{NP}}^2} \right), \quad (33)$$

$$|f_{tb}^{(8)}| \simeq \frac{9\pi}{2} \left(\frac{m_t^2}{\Lambda_{\text{NP}}^2} \right), \quad (34)$$

$$|f_{qq}| \simeq \frac{32\pi}{7} \left(\frac{m_t^2}{\Lambda_{\text{NP}}^2} \right), \quad (35)$$

$$|f_{qq}^{(8)}| \simeq 6\pi \left(\frac{m_t^2}{\Lambda_{\text{NP}}^2} \right), \quad (36)$$

³For a possibly less strong constraint on \mathcal{O}_{DW} and \mathcal{O}_{DB} see [16,17].

⁴In the expression for $\mathcal{O}_{tG\Phi}$ we assumed $\Lambda_{\text{NP}} \sim 10$ TeV. Our results are derived by considering four-body amplitudes at the tree approximation. This may not be adequate for \mathcal{O}_{t1} which is given by the standard top Yukawa interaction multiplied by $\Phi^\dagger \Phi$. This problem is not further investigated though, since \mathcal{O}_{t1} never contributes to the processes studied here.

$$|f_{t1}| \approx \frac{16\pi}{3\sqrt{2}} \left(\frac{m_t^2}{v\Lambda_{\text{NP}}} \right), \quad (37)$$

$$|f_{t2}| \approx 8\pi\sqrt{3} \left(\frac{m_t^2}{\Lambda_{\text{NP}}^2} \right), \quad (38)$$

$$|f_{t3}| \approx 8\pi\sqrt{6} \left(\frac{m_t^2}{\Lambda_{\text{NP}}^2} \right), \quad (39)$$

$$|f_{D_t}| \approx 10.4 \left(\frac{m_t^2}{\Lambda_{\text{NP}}^2} \right) \text{ for } f_{D_t} > 0, \\ |f_{D_t}| \approx -6.4 \left(\frac{m_t^2}{\Lambda_{\text{NP}}^2} \right) \text{ for } f_{D_t} < 0, \quad (40)$$

$$|f_{tW\Phi}| \approx \frac{61.6}{\sqrt{1+645(m_t^2/\Lambda_{\text{NP}}^2)}} \left(\frac{m_t^2}{\Lambda_{\text{NP}}^2} \right), \quad (41)$$

$$|f_{tB\Phi}| \approx \frac{61.6}{\sqrt{1+645m_t^2/\Lambda_{\text{NP}}^2}} \left(\frac{m_t^2}{\Lambda_{\text{NP}}^2} \right), \quad (42)$$

$$|f_{tG\Phi}| \approx \frac{m_t^2 \sqrt{\pi}}{v\Lambda_{\text{NP}} \sqrt{1 + \frac{2}{3}\alpha_s}}. \quad (43)$$

At present the most important constraints on these couplings arise from the Z-peak experiments at LEP 1 and SLC [20,16]. In the near future the process $e^+e^- \rightarrow W^+W^-$ at LEP 2, is expected to give direct constraints on the bosonic operators in Eqs. (17)–(19) [11,10]. In addition, if the Higgs boson is light enough, the processes $e^+e^- \rightarrow HZ$ and $e^+e^- \rightarrow H\gamma$ will also produce constraints on the three other bosonic operators (20)–(22) [12]. In Sec. VI, all these constraints will be presented together with the observability limits that could be derived from the $e^-e^+ \rightarrow t\bar{t}$ and $t \rightarrow bW$ processes.

III. $e^-e^+ \rightarrow t\bar{t}$ AMPLITUDE

As has been mentioned in the Introduction, box diagrams are never important for calculating the leading NP effects in $e^-e^+ \rightarrow t\bar{t}$. The amplitude has therefore a tree-level structure with γ and Z exchange in the s channel. Therefore, we only need to determine the $Vt\bar{t}$ ($V = \gamma, Z$) vertex, whose most general CP -conserving form is

$$-i\epsilon_\mu^V J_V^\mu = -ie_v \epsilon_\mu^V u_t(p) [\gamma^\mu d_1^V(q^2) + \gamma^\mu \gamma^5 d_2^V(q^2) \\ + (p-p')^\mu d_3^V(q^2)] v_{\bar{t}}(p'), \quad (44)$$

where ϵ_μ^V is the polarization of the vector boson V . The outgoing momenta (p, p') refer to (t, \bar{t}) , respectively, and satisfy $q \equiv p + p'$. The normalizations are determined by $e_\gamma \equiv e$ and $e_Z \equiv e/(2s_W c_W)$. The couplings d_i^V are in general q^2 -dependent form factors. The contributions to these from the SM at the tree level are

$$d_1^{\gamma, \text{SM}0} = \frac{2}{3}, \quad d_1^{Z, \text{SM}0} = g_{Vt} = \frac{1}{2} - \frac{4}{3}s_W^2, \\ d_2^{Z, \text{SM}0} = -g_{At} = -\frac{1}{2}. \quad (45)$$

In addition, there exist SM contributions to these couplings at the one-loop level, $d_i^{V, \text{SM}1}$, whose leading large m_t part is computed in Sec. V. Finally in Sec. VI we calculate the leading NP contributions to d_i^V . For the operators (\mathcal{O}_{t2} , \mathcal{O}_{D_t} , $\mathcal{O}_{tW\Phi}$, $\mathcal{O}_{tB\Phi}$), these arise at the tree level. For (\mathcal{O}_{qt} , $\mathcal{O}_{qt}^{(8)}$, \mathcal{O}_{tt} , \mathcal{O}_{tb} , $\mathcal{O}_{tG\Phi}$) and the six purely bosonic operators (\mathcal{O}_W , $\mathcal{O}_{W\Phi}$, $\mathcal{O}_{B\Phi}$, \mathcal{O}_{UW} , \mathcal{O}_{UB} , $\mathcal{O}_{\Phi 2}$) we need to go to the one-loop level in order to find a nonvanishing leading-logarithmic contribution which is also enhanced by a power of m_t^2 . Finally, for the operators $\mathcal{O}_{tb}^{(8)}$, \mathcal{O}_{qq} , $\mathcal{O}_{qq}^{(8)}$, \mathcal{O}_{t1} , and \mathcal{O}_{t3} we get no such leading NP contribution, up to the one-loop order.

The $e^-e^+ \rightarrow t\bar{t}$ helicity amplitude is written as $F_{\lambda, \tau, \tau'}$, where $\lambda \equiv \lambda(e^-) = -\lambda'(e^+) = \pm 1/2$ denote the e^- , e^+ helicities, while τ and τ' represent, respectively, the t and \bar{t} helicities. For completeness we also mention that the (e^-, e^+) incoming momenta are denoted as (k, k') , while the (t, \bar{t}) outgoing momenta are (p, p') . Using the couplings defined in Eq. (44), we write

$$F_{\lambda, \tau, \tau'} = \sum_{V=\gamma, Z} 2\lambda e^2 \sqrt{s} (A_V - 2\lambda B_V) \{ d_1^V [2m_t \sin\theta \delta_{\tau\tau'} \\ + \sqrt{s} \cos\theta (\tau' - \tau) - 2\lambda \sqrt{s} \delta_{\tau, -\tau'}] \\ - d_2^V 2|\vec{p}| [\cos\theta \delta_{\tau, -\tau'} + 2\lambda (\tau - \tau')] \\ - d_3^V 4|\vec{p}|^2 \sin\theta \delta_{\tau\tau'} \}, \quad (46)$$

with $A_\gamma = -1/s$, $A_Z = g_{Ve}/(4s_W^2 c_W^2 D_Z)$, $B_\gamma = 0$, $B_Z = g_{Ae}/(4s_W^2 c_W^2 D_Z)$, $g_{Ve} = -1/2 + 2s_W^2$, $g_{Ae} = -1/2$, and $D_Z = s - M_Z^2 + iM_Z\Gamma_Z$. In Eq. (46), θ is the (e^-, t) scattering angle in the (e^-, e^+) c.m. frame. The amplitude is normalized so that the unpolarized $e^-e^+ \rightarrow t\bar{t}$ differential cross section is given by

$$\frac{d\sigma(e^-e^+ \rightarrow t\bar{t})}{d\cos\theta} = \frac{3\beta_t}{128\pi s} \sum_{\lambda, \tau, \tau'} |F_{\lambda, \tau, \tau'}|^2, \quad (47)$$

where $\beta_t = (1 - 4m_t^2/s)^{1/2}$ and the color factor has been included. We note that CP invariance implies [21]

$$F_{\lambda, \tau, \tau'} = F_{\lambda, -\tau', -\tau}, \quad (48)$$

which is of course satisfied by Eq. (46). In fact, at the level of approximations used in constructing Eq. (46), CPT implies also

$$F_{\lambda, \tau, \tau'} = F_{\lambda, -\tau', -\tau}^*, \quad (49)$$

which indicates that all helicity amplitudes must be real.

Because of CP and CPT symmetries, it turns out that the simple t (or \bar{t}) decay distribution contains all the information that can be extracted from the amplitudes in Eq. (46). Thus, nothing more can be learned by considering the combined decay distributions of t and \bar{t} simultaneously. It is, therefore,

sufficient to consider only the simple spin density matrix of the produced t or \bar{t} . For the top quark, this is

$$\rho_{\tau_1 \tau_2}^{L,R} = \sum_{\tau'} F_{\lambda, \tau_1, \tau'} F_{\lambda, \tau_2, \tau'}^* \quad (50)$$

where L, R correspond, respectively, to $\lambda \equiv \lambda(e^-) = -\lambda'(e^+) = \mp 1/2$. There are only six independent elements (real in our case) $\rho_{++}^{L,R}$, $\rho_{--}^{L,R}$, and $\rho_{+-}^{L,R} = \rho_{-+}^{L,R}$, which can be measured through the top quark production and decay distributions. Each ρ element has a typical angular distribution given in terms of the form $(1 + \cos^2\theta)$, $\sin^2\theta$, and $\cos\theta$, producing symmetrical and asymmetrical θ distributions. Combining this with the decay angular information, various ρ elements can be isolated. Performing such measurements at a few e^-e^+ energies, even for unpolarized beams, one can define a sufficient number of independent quantities that can be used to determine the six couplings d_i^V , $V = \gamma, Z$, $i = 1, 3$. Many of these quantities (and in particular those of interest here) are forward-backward asymmetries in the angular distribution of physical observables concerning the produced top quark. QCD effects to these observables are probably small [19,22], and in any case they should be incorporated in our formalism in the future.

Electron beam polarization should provide an independent and maybe cleaner way to disentangle these couplings, through the separation of left-handed ($L \Leftrightarrow \lambda = -1/2$) and right-handed ($R \Leftrightarrow \lambda = +1/2$) contributions. Thus, in addition to the unpolarized quantities, we would then also have the $L-R$ ones. This way, the information from the usual unpolarized $L+R$ integrated cross section $\sigma(e^-e^+ \rightarrow t\bar{t})$ will be augmented by the availability of also σ^L and σ^R , allowing us to measure the integrated left-right asymmetry A_{LR} defined as $(\sigma^L - \sigma^R)/(\sigma^L + \sigma^R)$. Similarly, any forward-backward asymmetry constructed for the unpolarized ($L+R$) case will be accompanied by the corresponding one in the polarized ($L-R$) case. Details are given in Appendix B, where we thus define the six forward-backward asymmetries A_{FB} , $A_{FB, \text{pol}}$, H_{FB} , $H_{FB, \text{pol}}$, T_{FB} , and $T_{FB, \text{pol}}$.

IV. $t \rightarrow Wb$ DECAY AMPLITUDES AND INDUCED ASYMMETRIES

The $t(p_t) \rightarrow W^+(p_W)b(p_b)$ decay, where (p_t, p_W, p_b) are the related momenta, will be used to construct the asymmetries mentioned in the last paragraph of the previous section which are sensitive to the NP couplings affecting the $e^-e^+ \rightarrow t\bar{t}$ and to (a lesser extent) the ones determining $t \rightarrow bW$. To describe the NP effects in the t decay, we write the general $t \rightarrow W^+b$ vertex in terms of four invariant couplings, related through CPT invariance to the other four invariant couplings for $\bar{t} \rightarrow W^- \bar{b}$. These couplings are given by

$$\begin{aligned} -i \epsilon_\mu^{W*} J_W^\mu = & -i \frac{g V_{tb}^*}{2\sqrt{2}} \epsilon_\mu^{W*} \bar{u}_b(p_b) [\gamma^\mu d_1^W + \gamma^\mu \gamma^5 d_2^W \\ & + (p_t + p_b)^\mu d_3^W + (p_t + p_b)^\mu \gamma^5 d_4^W] u_t(p_t), \end{aligned} \quad (51)$$

where ϵ_μ^{W*} is the W polarization vector and V_{tb}^* is the appropriate CKM matrix element. The couplings d_i^W receive contributions from SM and NP. The *tree level SM contribution* is

$$d_1^{W, \text{SM}0} = -d_2^{W, \text{SM}0} = 1, \quad d_3^{W, \text{SM}0} = d_4^{W, \text{SM}0} = 0. \quad (52)$$

The *one-loop m_t^2 -enhanced SM contributions* $d_i^{W, \text{SM}1}$ are computed in Sec. V and they also satisfy the relations

$$d_1^{W, \text{SM}} = -d_2^{W, \text{SM}}, \quad d_3^{W, \text{SM}} = d_4^{W, \text{SM}}. \quad (53)$$

Finally the NP contributions to top quark decay are also given in Appendix B and collected in Sec. VI. Here we only note that the operators (\mathcal{O}_{t3} , \mathcal{O}_{Dt} , $\mathcal{O}_{tW\Phi}$) contribute already at the tree level, while \mathcal{O}_{qq} , $\mathcal{O}_{qq}^{(8)}$, $\mathcal{O}_{tG\Phi}$, $\mathcal{O}_{W\Phi}$, $\mathcal{O}_{B\Phi}$, \mathcal{O}_{UW} , and $\mathcal{O}_{\Phi 2}$ supply one-loop ‘‘leading-logarithmic’’ contributions, enhanced by powers of m_t^2 . The remaining \mathcal{O}_{qt} , $\mathcal{O}_{qt}^{(8)}$, \mathcal{O}_{tt} , \mathcal{O}_{tb} , $\mathcal{O}_{tb}^{(8)}$, \mathcal{O}_{t1} , \mathcal{O}_{t2} , $\mathcal{O}_{tB\Phi}$, \mathcal{O}_W , and \mathcal{O}_{UB} give no such contribution to $t \rightarrow bW$, up to this order.

In Appendix B we give the explicit forms of the asymmetry observables, sensitive to the production couplings defined in Eq. (44) and the decay ones in Eq. (51). Since we expect the NP effects to be small, we are only interested in observables that are sensitive to the interferences between the NP and the tree-level SM effects. Below, we first comment on the asymmetries sensitive to the decay couplings and then on the production ones.

The $t \rightarrow bW^+ \rightarrow bl^+ \nu$ observables which are interesting to measure are those sensitive to the interference between the NP and the tree-level SM effects. It turns out that these depend only on the combinations $(d_1^{W, \text{NP}} - d_2^{W, \text{NP}})$ and $(d_3^{W, \text{NP}} + d_4^{W, \text{NP}})$. The $d_{3,4}^W$ couplings have the peculiarity of leading only to a W , longitudinally polarized along the t quark momentum, whereas $d_{1,2}^W$ contribute to both the transverse and longitudinal W 's. Because of this, only the combination $(d_3^{W, \text{NP}} + d_4^{W, \text{NP}})$ can contribute linearly to the asymmetries relevant for the top quark decay distribution. In Appendix B, two versions of such an asymmetry are given, referring to the angular distribution of the lepton coming from the semileptonic t or \bar{t} decay.

The other combination $(d_1^{W, \text{NP}} - d_2^{W, \text{NP}})$ cannot be seen at linear order through asymmetries. For a physical quantity sensitive to it, we have to look at the partial width $\Gamma(t \rightarrow Wb)$:

$$\begin{aligned} \Gamma(t \rightarrow Wb) = & \frac{G_F |V_{tb}^*|^2 (m_t^2 - M_W^2)^2}{16\pi \sqrt{2} m_t^3} \\ & \times \{ [(d_1^W)^2 + (d_2^W)^2] (m_t^2 + 2M_W^2) \\ & + [(d_3^W)^2 + (d_4^W)^2] (m_t^2 - M_W^2)^2 \\ & + 2[d_3^W d_1^W - d_4^W d_2^W] m_t (m_t^2 - M_W^2) \}, \end{aligned} \quad (54)$$

where it appears multiplied by the CKM matrix element also. Unfortunately, the width $\Gamma(t \rightarrow Wb)$ cannot be directly measured to the necessary accuracy. Only indirectly can this be done, either using the fusion process $W\gamma \rightarrow tb$ accessible at an e^-e^+ collider in the $e\gamma$ mode (through laser backscatter-

ing) or using reactions such as $q\bar{q}' \rightarrow t\bar{b}$ and $Wg \rightarrow t\bar{b}$ accessible at the Fermilab Tevatron and CERN Large Hadron Collider (LHC) colliders, respectively. For such a measurement, one can expect an accuracy of only about 20–30 % for $(d_1^{W,\text{NP}} - d_2^{W,\text{NP}})$ [23,24].

We next turn to the asymmetries sensitive to the production couplings defined in Eq. (44). For constructing them, we need a description of the angular distribution of top quark production and decay. Below, we only give expressions for completely longitudinally polarized beams. In such a case, the angular distribution for $e^-e^+ \rightarrow t\bar{t}(t \rightarrow bW \rightarrow bl\nu)$ can be written as

$$\frac{d\sigma^{L,R}}{d\cos\theta} = \frac{3\beta_t}{32\pi s} \sum_{\tau_1\tau_2\tau'} F_{\lambda\tau_1\tau'} F_{\lambda\tau_2\tau'}^* t_{\tau_1\tau_2}, \quad (55)$$

where (L,R) correspond to $\lambda \equiv \lambda(e^-) = -\lambda'(e^+) = \mp 1/2$, respectively, and $t_{\tau_1\tau_2}$ is the t -quark-decay matrix constructed in terms of the helicity amplitude $\mathcal{M}_\tau(t \rightarrow bW^+ \rightarrow bl^+\nu)$, with τ being the top quark helicity. We thus have

$$t_{\tau_1\tau_2} = \frac{(2\pi)^4}{2m_t\Gamma_t} \sum_{\text{spins}} \mathcal{M}_{\tau_1} \mathcal{M}_{\tau_2}^* d\Phi_3(bl\nu), \quad (56)$$

where Γ_t is the total top quark width, \sum_{spins} means summation over the final (b, l^+, ν) spins, and $d\Phi_3(bl\nu)$ is the usual three-body phase space describing t quark decay in its rest frame [25].

It is convenient to express the three-body phase space in terms of the Euler angles determining the t -quark-decay plane. We start from the process $e^-(k)e^+(k') \rightarrow t(p)\bar{t}(p')$ in the center-of-mass frame, where with θ we denote the (e^-, t) scattering angle. The t quark rest frame (called the t frame hereafter) is then defined with its z axis along the top quark momentum; the x axis is taken in the $(t\bar{t})$ production plane, so that the y axis is perpendicular to it and along the direction of $\vec{k} \times \vec{p}'$ of the e^- and t momenta. In this t frame we define the top quark decay plane through the Euler angles $(\varphi_1, \vartheta_1, \psi_1)$ described in Appendix B. In addition, within the top quark decay plane we define θ_l as the angle between the lepton momentum and the top quark momentum, after having boosted to the W rest frame [19]. It is related to the l^+ energy in the t frame by

$$E_l = |\vec{p}_l| = \frac{m_t^2 + M_W^2 - \cos\theta_l(m_t^2 - M_W^2)}{4m_t}, \quad (57)$$

where the (b, l^+) masses are neglected. In terms of the Euler angles, the three-body phase space becomes [25]

$$\begin{aligned} \delta[(p_l + p_\nu)^2 - M_W^2] d\Phi_3(bl\nu) \\ \Rightarrow \frac{(m_t^2 - M_W^2)}{64m_t^2(2\pi)^9} d\varphi_1 d\cos\vartheta_1 d\psi_1 d\cos\theta_l, \end{aligned} \quad (58)$$

after including the constraint that the $l\nu$ pair lie at the W mass shell. Like ρ , the matrix $t_{\tau_1\tau_2}$ also involves three real independent elements $(\tau_1\tau_2) = (++)$, $(--)$, and $(+-)$. They are explicitly written in terms of the above angles in

Appendix B. Using these, we construct the three forward-backward asymmetries for the unpolarized case $(L+R)$ and another three for the polarized one $(L-R)$, which can be used to measure the production couplings in Eq. (44).

V. LEADING m_t -ENHANCED SM CONTRIBUTIONS AT ONE LOOP

In the present section we study the one-loop, m_t -enhanced SM contributions to $e^-e^+ \rightarrow t\bar{t}$ and $t \rightarrow bW$. Technically this means that we consider the large- m_t limit of the one-loop diagrams, keeping m_H/m_t and $s/m_t^2 \equiv q^2/m_t^2$ finite. Such a study is useful for checking the possible appearance of any large- m_t effect. It is also instructive for comparison with the corresponding NP effects. The relevant diagrams supplying such m_t^2 enhancements consist of triangular vertex diagrams for the $\gamma t\bar{t}$, $Zt\bar{t}$, and Wtb vertices, and also of the t and b self-energy diagrams, involving exchanges of Goldstone bosons and physical Higgs bosons. Diagrams involving gauge boson exchanges, or box diagrams, cannot generate m_t^2 enhancements. We have checked that these contributions to the form factors in Eqs. (44) and (51) are gauge invariant and determine the complete SM large- q^2 , large- m_t effect in $e^-e^+ \rightarrow t\bar{t}$ and $t \rightarrow bW$. Note that we leave aside the gauge boson (γ, Z, W) self-energy contributions which are universal (i.e., not related to the $t\bar{t}$ channel) and are taken into account in the usual renormalization procedure [26]. For $q^2 \sim 4m_t^2$, the resulting one-loop contributions to the form factors defined in Eq. (44) are given by

$$d_1^{\gamma,\text{SM1}}(q^2) = -C \left[\frac{8+I_{se}}{3} + \frac{1}{3}I_0 - \frac{1}{6}J_1 + \frac{1}{3}(I_2+I_{2H}) - \frac{2}{3}J_{4H} \right], \quad (59)$$

$$d_2^{\gamma,\text{SM1}}(q^2) = -C \left[\frac{1}{3} + \frac{1}{3}I_0 + \frac{1}{6}J_1 \right], \quad (60)$$

$$d_3^{\gamma,\text{SM1}}(q^2) = \frac{2C}{3m_t} \left[\frac{1}{2}J_{2H} - J_0 \right], \quad (61)$$

$$\begin{aligned} d_1^{Z,\text{SM1}}(q^2) = C \left[-\frac{3+I_{se}}{4} + \frac{2s_W^2}{3}(8+I_{se}) + \frac{2s_W^2}{3}I_0 \right. \\ \left. + \frac{1}{2} \left(1 - \frac{2s_W^2}{3} \right) J_1 - \frac{1}{4} \left(1 - \frac{8s_W^2}{3} \right) \right. \\ \left. \times (I_2 + I_{2H} - 2J_{4H}) \right], \end{aligned} \quad (62)$$

$$\begin{aligned} d_2^{Z,\text{SM1}}(q^2) = C \left[\frac{3+I_{se}}{4} + \frac{2s_W^2}{3} + \frac{2s_W^2}{3}I_0 - \frac{1}{2} \left(1 - \frac{2s_W^2}{3} \right) J_1 \right. \\ \left. + I_{1H} - \frac{1}{4}(I_2 + I_{2H}) + \frac{1}{2}J_{3H} \right], \end{aligned} \quad (63)$$

$$d_3^{Z,\text{SM1}}(q^2) = \frac{C}{m_t} \left[\frac{1}{4} \left(1 - \frac{8s_W^2}{3} \right) J_{2H} - \left(1 - \frac{4s_W^2}{3} \right) J_0 \right], \quad (64)$$

with $C = g^2 m_t^2 / (64\pi^2 M_W^2)$, and

$$\begin{aligned} I_{se} &= -2 \int_0^1 dx (1-x) \ln[x^2 + \zeta(1-x)] \\ &= 3 - 2\zeta \left(1 - \frac{\zeta}{4} \right) \ln(\zeta) - \zeta - (\zeta - 2) \sqrt{\zeta(\zeta - 4)} - i\epsilon \\ &\quad \times \operatorname{arccosh} \left(\frac{\sqrt{\zeta}}{2} - i\epsilon \right), \end{aligned} \quad (65)$$

$$I_0 = 2 \int_0^1 dx_1 \int_0^{1-x_1} dx_2 \ln[(x_1 + x_2)(x_1 + x_2 - 1) - 4\eta x_1 x_2], \quad (66)$$

$$I_{1H} = 2 \int \int dx_1 dx_2 \ln[(x_1 + x_2 - 1)^2 - 4\eta x_1 x_2 + \zeta x_1], \quad (67)$$

$$I_2 = 2 \int \int dx_1 dx_2 \ln[(x_1 + x_2)^2 - 4\eta x_1 x_2], \quad (68)$$

$$\begin{aligned} I_{2H} &= 2 \int \int dx_1 dx_2 \ln[(x_1 + x_2)^2 - 4\eta x_1 x_2 \\ &\quad + \zeta(1 - x_1 - x_2)], \end{aligned} \quad (69)$$

$$J_0 = 2 \int \int dx_1 dx_2 \frac{(x_1 + x_2)(x_1 + x_2 - 1)}{(x_1 + x_2)(x_1 + x_2 - 1) - 4\eta x_1 x_2}, \quad (70)$$

$$J_1 = 2 \int \int dx_1 dx_2 \frac{(x_1 + x_2 - 1)}{(x_1 + x_2)(x_1 + x_2 - 1) - 4\eta x_1 x_2}, \quad (71)$$

$$\begin{aligned} J_{2H} &= 2 \int \int dx_1 dx_2 \left[\frac{(x_1 + x_2)(x_1 + x_2 - 2)}{(x_1 + x_2)^2 - 4\eta x_1 x_2 + \zeta(1 - x_1 - x_2)} \right. \\ &\quad \left. + \frac{(x_1 + x_2)^2}{(x_1 + x_2)^2 - 4\eta x_1 x_2} \right], \end{aligned} \quad (72)$$

$$J_{3H} = 2 \int \int dx_1 dx_2 \frac{2[1 - (\zeta/4)(x_1 + x_2 - 1)]}{(x_1 + x_2)^2 - 4\eta x_1 x_2 + \zeta(1 - x_1 - x_2)}, \quad (73)$$

$$J_{4H} = 2 \int \int dx_1 dx_2 \frac{2 - (\zeta/2)(x_1 + x_2 - 1)}{(x_1 + x_2)^2 - 4\eta x_1 x_2 + \zeta(1 - x_1 - x_2)}, \quad (74)$$

with $\eta = (q^2 + i\epsilon)/(4m_t^2)$ and $\zeta = m_H^2/m_t^2$. The double integration runs over the interval $[0,1]$ for x_1 and $[0,1-x_1]$ for x_2 . These integrals have been computed partially analytically and partially numerically.⁵

It can be noted from these results that close to threshold (i.e., $q^2 \sim 4m_t^2$), there is a rather strong m_t^2/m_H^2 dependence arising from the triangle diagrams involving physical Higgs boson exchange. If we put $m_t \gg m_H$, then the SM contribu-

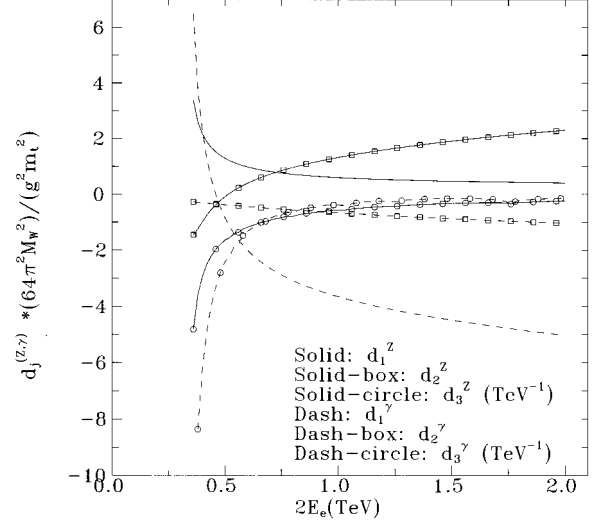


FIG. 1. One-loop SM contributions to the d_j^γ and d_j^Z form factors defined in Eq. (44), as functions of $\sqrt{q^2} = 2E_e$.

tion acquires infrared-type singularities, which are obviously related to the stability of scalar sector requiring $m_t \sim m_H$ for physically acceptable m_t masses [27].

In Fig. 1 we plot (in units of the coefficient $C \approx 0.003$) these SM contributions to the six form factors, as functions of $\sqrt{q^2} \equiv (2E_e)$, for $m_H = 0.1$ TeV and $q^2 > 4m_t^2$. For $q^2 \sim (0.5 \text{ TeV})^2$ we find from this figure an effect of the order of 1% for the vector γtt coupling and of the order of 3 per mille for the other vector and axial couplings. The ‘‘derivative’’ $d_3^{\gamma,Z}$ couplings are somewhat weaker.

We next turn to the m_t^2 -enhanced SM corrections to the $t \rightarrow bW$ decay. The resulting one-loop contributions, expressed in terms of the decay couplings defined in Eq. (51), is

$$d_1^{W,SM1} = -d_2^{W,SM1} = -C \left[\frac{5}{4} + \frac{1}{4} I_{se} + \frac{1}{2} H_1 \right], \quad (75)$$

$$d_3^{W,SM1} = d_4^{W,SM1} = -\frac{C}{2m_t} [1 + H_2], \quad (76)$$

where

$$H_1 = 2 \int \int dx_1 dx_2 \ln[x_1(x_1 + x_2) - \zeta(x_1 + x_2 - 1)], \quad (77)$$

$$H_2 = 2 \int \int dx_1 dx_2 \frac{x_1(x_1 + x_2 - 2)}{x_1(x_1 + x_2) - \zeta(x_1 + x_2 - 1)}. \quad (78)$$

For $m_H = 0.1$ TeV these equations give

$$d_1^{W,SM1} = -d_2^{W,SM1} = C(-0.92), \quad (79)$$

$$d_3^{W,SM1} = d_4^{W,SM1} = C \left(\frac{0.0728}{2m_t} \right). \quad (80)$$

Comparing the definition of the various couplings given in

⁵We thank N.D. Vlachos for his help in this numerical computation.

Eq. (51), with relations (75) and (76), we remark that the SM m_t^2 -enhanced couplings only affect the left-handed b_L field. This is also obvious from the structure of the relevant diagrams.

VI. NP EFFECTS

In Appendix A we enumerate the relevant diagrams giving the leading NP contribution to $e^-e^+ \rightarrow t\bar{t}$ and $t \rightarrow bW$, for each kind of operator. Since box diagrams are never important, the leading NP contribution to $e^-e^+ \rightarrow t\bar{t}$ can be expressed in terms of the NP contributions to the form factors introduced in Eq. (44). Here, $s = q^2 \geq 4m_t^2$ is understood. As already stated, the operators (\mathcal{O}_{t2} , \mathcal{O}_{Dt} , $\mathcal{O}_{tW\Phi}$, $\mathcal{O}_{tB\Phi}$) give tree-level contributions, which are

$$d_1^{\gamma, \text{NP}}(s) = -\frac{4\sqrt{2}M_W}{e^2m_t}(s_W^2 f_{tW\Phi} + s_W c_W f_{tB\Phi}), \quad (81)$$

$$d_3^{\gamma, \text{NP}}(s) = \frac{2\sqrt{2}M_W}{e^2m_t^2}(s_W^2 f_{tW\Phi} + s_W c_W f_{tB\Phi}), \quad (82)$$

$$d_1^{Z, \text{NP}}(s) = -\frac{2M_W^2}{g^2m_t^2}f_{t2} + \frac{8\sqrt{2}M_W}{g^2m_t}(c_W^2 f_{tW\Phi} + s_W c_W f_{tB\Phi}), \quad (83)$$

$$d_2^{Z, \text{NP}}(s) = -\frac{2M_W^2}{g^2m_t^2}f_{t2}, \quad (84)$$

$$d_3^{Z, \text{NP}}(s) = -\frac{M_W}{\sqrt{2}gm_t^2}f_{Dt} + \frac{4\sqrt{2}M_W}{g^2m_t^2}(c_W^2 f_{tW\Phi} - s_W c_W f_{tB\Phi}). \quad (85)$$

We next turn to the operators contributing only at the one-loop level. As explained above, we consider only the leading NP effect determined by the divergent part⁶ of the Feynman integrals, provided it is enhanced by some power of m_t^2 . The contributions from the ‘‘top’’-involving operators are then expressed in terms of

$$F_i \equiv \frac{1}{16\pi^2} \ln\left(\frac{\Lambda^2}{\mu^2}\right) \frac{f_i}{m_t^2}, \quad (86)$$

with Λ being the divergent integral cutoff identified with the NP scale Λ_{NP} and $\mu \sim \sqrt{s}$ being the scale where the effective coupling is measured. For the purely bosonic operators, due to their different normalization implied by (24) and (25), we should replace in Eq. (86) $f_i/m_t^2 \rightarrow (\lambda_W/M_W^2, f_W/M_W^2, f_B/M_W^2, d/v^2, d_B/v^2, f_{\Phi 2}/v^2)$ for ($\mathcal{O}_W, \mathcal{O}_{W\Phi}, \mathcal{O}_{B\Phi}, \mathcal{O}_{UW}, \mathcal{O}_{UB}, \mathcal{O}_{\Phi 2}$), respectively. We thus get

$$d_1^{\gamma, \text{NP}}(s) = \frac{s}{6}F_{qt} + \frac{8s}{9}F_{qt(8)} - \frac{8s}{9}F_{tt} + \frac{s}{3}F_{tb} + \frac{256\sqrt{2}g_s m_t M_W}{9g}F_{tG\Phi} + \frac{g^2 s}{4}F_W - \frac{g^2 m_t^2 s}{32M_W^2} \times [F_{W\Phi} + F_{B\Phi}] - 2m_t^2 F_{UW} - \frac{10m_t^2}{3}F_{UB}, \quad (87)$$

$$d_2^{\gamma, \text{NP}}(s) = -\frac{s}{18}F_{qt} - \frac{8s}{27}F_{qt(8)} - \frac{8s}{9}F_{tt} + \frac{s}{3}F_{tb} - \frac{g^2 s}{4}F_W + \frac{g^2 m_t^2 s}{32M_W^2}[F_{W\Phi} - 3F_{B\Phi}], \quad (88)$$

$$d_3^{\gamma, \text{NP}}(s) = -\frac{128\sqrt{2}g_s M_W}{9g}F_{tG\Phi} + m_t F_{UW} + \frac{5m_t}{3}F_{UB}, \quad (89)$$

$$d_1^{Z, \text{NP}}(s) = -\frac{ss_W^2}{3}F_{qt} - \frac{16ss_W^2}{9}F_{qt(8)} - 4\left(m_t^2 - \frac{4ss_W^2}{9}\right)F_{tt} - \frac{2ss_W^2}{3}F_{tb} + \frac{64\sqrt{2}g_s(3-8s_W^2)m_t M_W}{9g}F_{tG\Phi} + \frac{sc_W^2 g^2}{2}F_W - \frac{g^2 m_t^2 s}{16M_W^2}[c_W^2 F_{W\Phi} - s_W^2 F_{B\Phi}] - 4m_t^2 c_W^2 F_{UW} + \frac{20m_t^2 s_W^2}{3}F_{UB}, \quad (90)$$

$$d_2^{Z, \text{NP}}(s) = -\left(m_t^2 - \frac{ss_W^2}{9}\right)F_{qt} - \left(\frac{16}{3}\right)\left(m_t^2 - \frac{ss_W^2}{9}\right)F_{qt(8)} - 4\left(m_t^2 - \frac{4ss_W^2}{9}\right)F_{tt} - \frac{2ss_W^2}{3}F_{tb} - \frac{sc_W^2 g^2}{2}F_W + \frac{g^2 m_t^2 s}{16M_W^2}[c_W^2 F_{W\Phi} + 3s_W^2 F_{B\Phi}] - 4m_t^2 F_{\Phi 2}, \quad (91)$$

$$d_3^{Z, \text{NP}}(s) = -\frac{32\sqrt{2}g_s(3-8s_W^2)M_W}{9g}F_{tG\Phi} + 2m_t c_W^2 F_{UW} - \frac{10m_t s_W^2}{3}F_{UB}. \quad (92)$$

Similarly, for the $t \rightarrow bW$ couplings defined in Eq. (51), the nonvanishing tree-level NP contributions are

$$d_1^{W, \text{NP}} = \frac{2M_W^2}{g^2 m_t^2} f_{t3} - \frac{4\sqrt{2}M_W}{g^2 m_t} f_{tW\Phi}, \quad (93)$$

$$d_2^{W, \text{NP}} = \frac{2M_W^2}{g^2 m_t^2} f_{t3} + \frac{4\sqrt{2}M_W}{g^2 m_t} f_{tW\Phi}, \quad (94)$$

⁶We always use dimensional regularization.

TABLE I. NP couplings and effects on production and decay observables.

\mathcal{O}_i	f_i, d, d_B, λ_W	$e^-e^+ \rightarrow t\bar{t}$	$\Gamma(t \rightarrow bW)$	D_{FB}^1	D_{FB}^2
<i>SM</i>		Yes	1.5581	0.2210	-0.5384
$+ \mathcal{O}_{qt}$	(+, -)1.8	Loop	No	No	No
$+ \mathcal{O}_{qt}^{(8)}$	(+, -)0.34	Loop	No	No	No
$+ \mathcal{O}_{tt}$	(+, -)0.27	Loop	No	No	No
$+ \mathcal{O}_{tb}$	(+, -)0.6	Loop	No	No	No
$+ \mathcal{O}_{tb}^{(8)}$		No	No	No	No
$+ \mathcal{O}_{qq}$	(+, -)3	No	1.5583	0.2210	-0.5384
$+ \mathcal{O}_{qq}^{(8)}$	(+, -)3	No	1.5644	0.2210	-0.5384, -0.5383
$+ \mathcal{O}_{t1}$		No	No	No	No
$+ \mathcal{O}_{t2}$	(+, -)0.12	Tree	No	No	No
$+ \mathcal{O}_{t3}$	(+, -)0.9	No	2.7910	0.2211	-0.5385, -0.5388
$+ \mathcal{O}_{Dt}$	(+, -)0.51	Tree	0.9373, 5.4581	0.2211	-0.5385
$+ \mathcal{O}_{tW\Phi}$	(-, +)0.012	Tree	1.6619, 1.4597	0.2407, 0.2030	-0.6720, -0.4491
$+ \mathcal{O}_{tB\Phi}$	(-, +)0.009	Tree	No	No	No
$+ \mathcal{O}_{tG\Phi}$	(+, -)0.24	Loop	1.5041, 1.6136	0.2117, 0.2313	-0.4860, -0.6034
$+ \mathcal{O}_W$	(+, -)0.40	Loop	No	No	No
$+ \mathcal{O}_{W\Phi}$	(-, +)0.63	Loop	1.5523, 1.5639	0.2219, 0.2202	-0.5433, -0.5336
$+ \mathcal{O}_{B\Phi}$	(-, +)0.75	Loop	1.5600, 1.5561	0.2207, 0.2214	-0.5365, 0.5404
$+ \mathcal{O}_{UW}$	(-, +)5.94	Loop	1.6770, 1.4463	0.2437, 0.2022	-0.6964, -0.4388
$+ \mathcal{O}_{UB}$	(-, +)5.35	Loop	No	No	No
$+ \mathcal{O}_{\Phi 2}$	(+, -)11.9	Loop	2.1235	0.2210	-0.5384

$$d_3^{W, \text{NP}} = \frac{4\sqrt{2}M_W}{g^2 m_t^2} f_{tW\Phi} - \frac{M_W}{g\sqrt{2}m_t^2} f_{Dt}, \quad (95)$$

$$d_4^{W, \text{NP}} = \frac{4\sqrt{2}M_W}{g^2 m_t^2} f_{tW\Phi} - \frac{M_W}{g\sqrt{2}m_t^2} f_{Dt}. \quad (96)$$

$$d_4^{W, \text{NP}} = \frac{m_t}{2} F_{qq} + \frac{8m_t}{3} F_{qq(8)} - \frac{32\sqrt{2}M_W g_s}{3g} F_{tG\Phi} - \frac{g^2 m_t (11s_W^2 - 6)}{24c_W^2} F_{W\Phi} - \frac{5g^2 m_t s_W^2}{24c_W^2} F_{B\Phi} + 2m_t F_{UW}. \quad (100)$$

Correspondingly, the nonvanishing one-loop m_t^2 -enhanced NP contributions (for the operators which do not have any tree-level ones) are

$$d_1^{W, \text{NP}} = \frac{m_t^2}{2} F_{qq} + \frac{8m_t^2}{3} F_{qq(8)} + \frac{32\sqrt{2}m_t M_W g_s}{3g} F_{tG\Phi} + \frac{g^2 m_t^2 (13s_W^2 - 3)}{48c_W^2} F_{W\Phi} + \frac{g^2 m_t^2 s_W^2}{48c_W^2} F_{B\Phi} - 2m_t^2 F_{UW} + 2m_t^2 F_{\Phi 2}, \quad (97)$$

$$d_2^{W, \text{NP}} = \frac{m_t^2}{2} F_{qq} + \frac{8m_t^2}{3} F_{qq(8)} - \frac{32\sqrt{2}m_t M_W g_s}{3g} F_{tG\Phi} - \frac{g^2 m_t^2 (13s_W^2 - 3)}{48c_W^2} F_{W\Phi} - \frac{g^2 m_t^2 s_W^2}{48c_W^2} F_{B\Phi} + 2m_t^2 F_{UW} - 2m_t^2 F_{\Phi 2}, \quad (98)$$

$$d_3^{W, \text{NP}} = -\frac{m_t}{2} F_{qq} - \frac{8m_t}{3} F_{qq(8)} - \frac{32\sqrt{2}M_W g_s}{3g} F_{tG\Phi} - \frac{g^2 m_t (11s_W^2 - 6)}{24c_W^2} F_{W\Phi} - \frac{5g^2 m_t s_W^2}{24c_W^2} F_{B\Phi} + 2m_t F_{UW}, \quad (99)$$

We now review the NP effects of each operator on the various observables. First note that the operators $\mathcal{O}_{tb}^{(8)}$ and \mathcal{O}_{t1} give no contribution (within our approximations) to either production or decay. The effects of the rest are illustrated in Table I, where we give the NP couplings used and the implications for the $t \rightarrow bW$ decay observables. The effects on top quark production through $e^-e^+ \rightarrow t\bar{t}$ are presented in ⁷ Figs. 2–9.

In order to make the production effects clearly visible in the figures, we have chosen the NP couplings such that the NP effect is about $\pm 30\%$ of the SM prediction on the integrated cross section. A corresponding choice with respect to the NP contribution to $\Gamma(t \rightarrow bW)$ has also been made for those operators which contribute only to decay and not to production. The third column in Table I identifies the operators giving a nonvanishing contribution to top quark production either at the tree or the one-loop level. The rest of the columns in Table I describe the NP effects on $\Gamma(t \rightarrow bW)$ and the two forward-backward asymmetries constructed in Appendix B for the semileptonic top quark decay.

⁷Note that in the figures, the signatures of $\mathcal{O}_{qt}^{(8)}$ are never shown explicitly, since they are identical to those from \mathcal{O}_{qt} , apart from an overall normalization factor of 16/3.

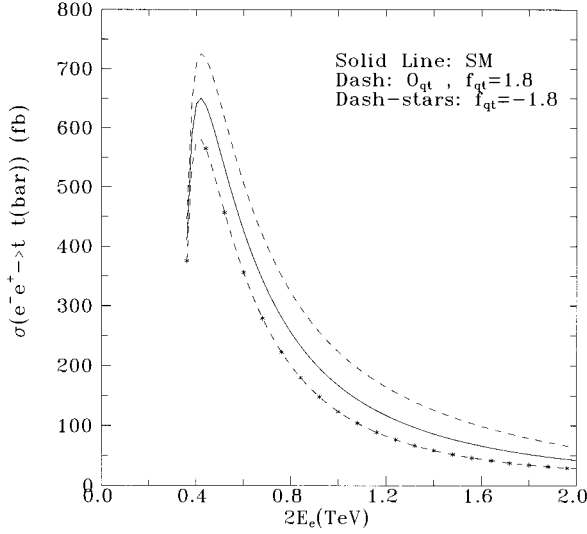


FIG. 2. NP effects for \mathcal{O}_{qt} as seen in the unpolarized cross section $\sigma(e^-e^+ \rightarrow t\bar{t})$, as a function of the c.m. energy $2E_e$. The indicated value of the f_{qt} coupling is chosen to create a 30% effect. Similar results are obtained for the contributing operators \mathcal{O}_{l2} , \mathcal{O}_{Dr} , $\mathcal{O}_{tW\Phi}$, $\mathcal{O}_{tB\Phi}$, $\mathcal{O}_{qt}^{(8)}$, \mathcal{O}_{ll} , \mathcal{O}_{lb} , $\mathcal{O}_{lG\Phi}$, and \mathcal{O}_W , $\mathcal{O}_{W\Phi}$, $\mathcal{O}_{B\Phi}$, \mathcal{O}_{UW} , \mathcal{O}_{UB} , and $\mathcal{O}_{\Phi 2}$, using the NP couplings shown in the second column of Table I.

In Fig. 2 we give the NP results for the integrated unpolarized cross section $\sigma(e^-e^+ \rightarrow t\bar{t})$ for the \mathcal{O}_{qt} case. Similar results would appear for all other operators if the associated coupling constants take the values given in Table I. The particular characteristics of each operator may then be studied by looking at the other observables appearing in the fourth to sixth columns of Table I and in Figs. 3–9. In detail, for unpolarized beams, the forward-backward asymmetry A_{FB} is illustrated in Fig. 3, the asymmetry H_{FB} in Fig. 4 and the asymmetry T_{FB} in Fig. 5. Correspondingly, for longitudinally polarized e^\mp beams, the asymmetry A_{LR} is illustrated in Fig. 6, while the forward-backward asymmetry $A_{FB,pol}$ is in Fig. 7, the asymmetry $H_{FB,pol}$ in Fig. 8 and $T_{FB,pol}$ in Fig. 9. Here, the (a) part of the figures refer to the four-quark operators, the (b) parts to the two-quark ones, and the (c) parts to the bosonic operators. Occasionally in the figures, the results for some operators or observables almost coincide for the couplings chosen above. Whenever this happens, it is just indicated in the figure caption.

The values for the coupling constants used in Table I, are often unacceptably large, either because of the existing indirect experimental constraints or because they would imply, through unitarity, a very low NP scale. Nevertheless, we used them in order to make the NP effects in the figures clearly visible.

The expected luminosity for a future linear collider is commonly taken as $80(\text{s/TeV}^2) \text{ fb}^{-1}/\text{yr}$. Since the SM cross section for $e^+e^- \rightarrow t\bar{t}$ is about $170 (\text{TeV}^2/\text{s}) \text{ fb}$, we expect a rate of more than 10^4 events/yr, implying a statistical accuracy of $\sim 1\%$ for the various physical quantities. The implied observability limits to various NP couplings are presented in Table II, where we also give the present constraints [20]. In getting them, we have always assumed that only one NP operator acts at a time. Moreover, we have conserva-

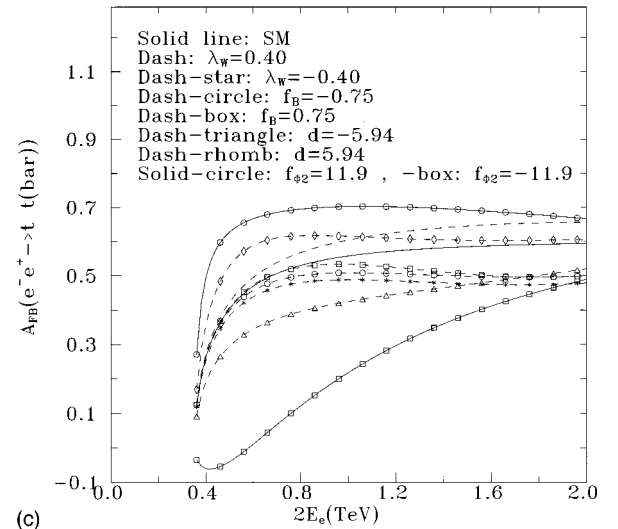
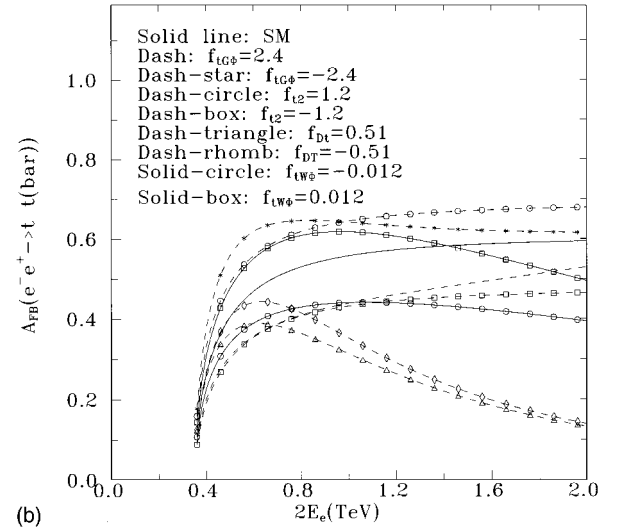
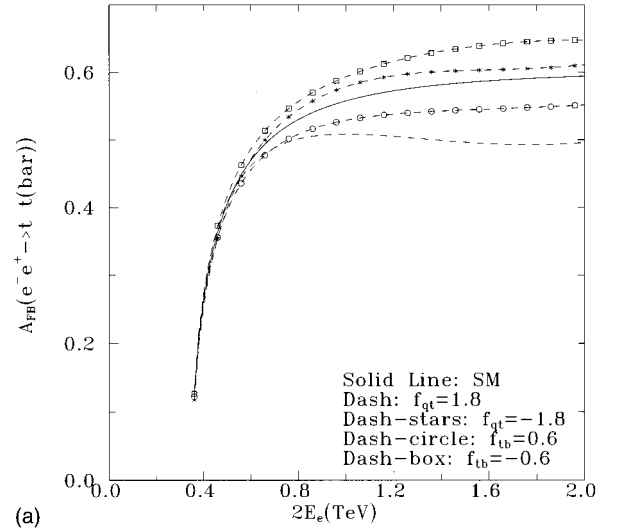


FIG. 3. NP effects on the unpolarized forward-backward asymmetry in the differential cross section $A_{FB}(e^-e^+ \rightarrow t\bar{t})$, as a function of the c.m. energy $2E_e$, for the NP couplings in Table I. (a) Four-quark NP operators; the \mathcal{O}_{ll} effect is similar to \mathcal{O}_{lb} . (b) Two-quark NP operators; $\mathcal{O}_{tB\Phi}$ gives similar effects to $\mathcal{O}_{tW\Phi}$. (c) Purely bosonic NP operators; the effects of $\mathcal{O}_{W\Phi}$ and \mathcal{O}_{UB} are similar to those from \mathcal{O}_W and \mathcal{O}_{UW} , respectively.

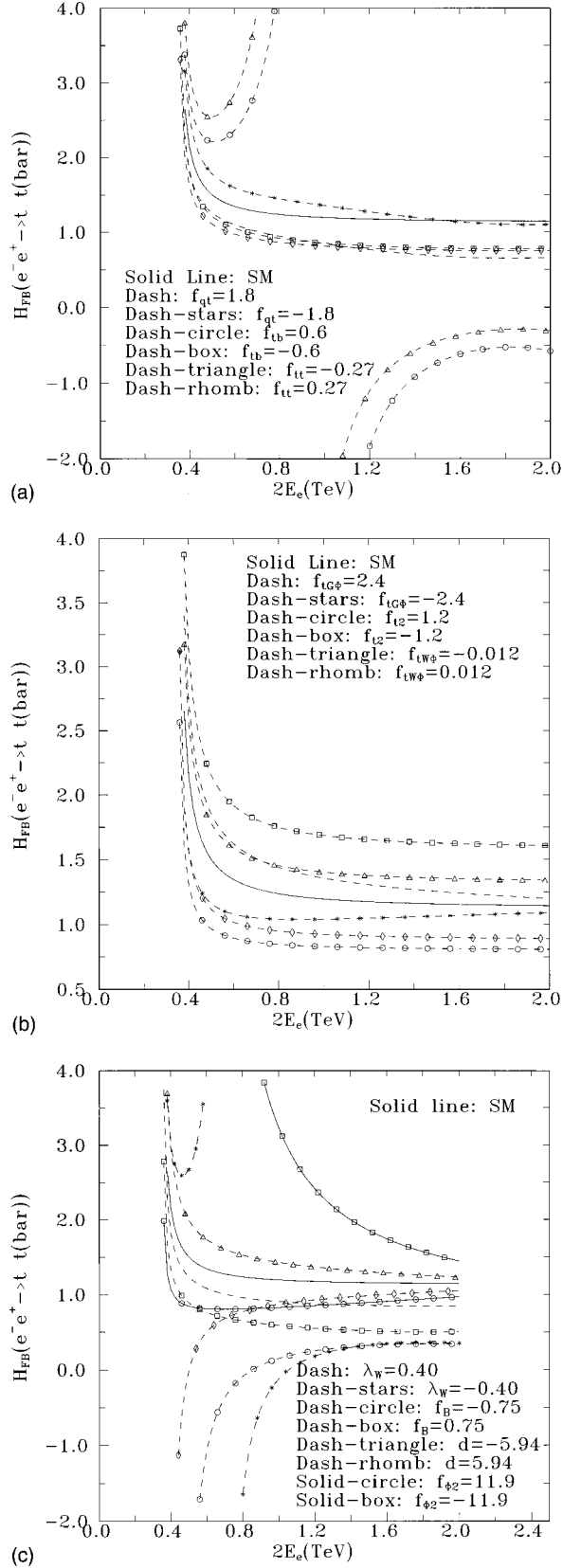


FIG. 4. NP effects on the unpolarized forward-backward asymmetry in the top quark average helicity $H_{\text{FB}}(e^+e^- \rightarrow t\bar{t})$, as a function of the c.m. energy $2E_e$, for the NP couplings in Table I. (a) Four-quark NP operators. (b) Two-quark NP operators; the $\mathcal{O}_{B\phi}$ effect is similar to 1/3 the one from $\mathcal{O}_{tW\phi}$, while the effect from \mathcal{O}_{D_t} is very small. (c) Purely bosonic operators; $\mathcal{O}_{W\phi}$ behaves similarly to \mathcal{O}_W , while \mathcal{O}_{UB} gives a very small contribution.

tively assumed a total (statistical + systematical) relative accuracy of 5% on the integrated cross section for unpolarized e^\pm beams and an absolute 5% accuracy on the asymmetries defined in Appendix B. More precise numbers require, of course, detailed Monte Carlo analyses, taking into account the precise experimental conditions. Finally, using the unitarity relations presented in Sec. II, we translate the observability limits on the various NP couplings to bounds on the highest related NP scales Λ_{NP} to which the specific measurements are sensitive. These bounds are also indicated in Table II. In the last three columns we have indicated, for each operator separately, the constraints established in Ref. [5] and the expected LEP 2 sensitivity. In all cases except for the $Z \rightarrow b\bar{b}$ case, the absolute value of the coupling constant is meant.

The following comments should now be made concerning the properties of the various operators and the observability limits presented in Table II.

A. Four-quark operators

\mathcal{O}_{qt} and $\mathcal{O}_{qt}^{(8)}$. Both operators lead to the same effects (apart from an overall normalization factor 16/3). They both contribute, at one loop, only to the vector and axial vector form factors $d_{1,2}^V$ and $d_{1,2}^Z$. They do not contribute to the top quark decay. So their modifications of the SM predictions are always rather uniform as one can see in the figures. The observability limits obtained either from the integrated cross section or from H_{FB} appear to be just marginally compatible with the LEP 1 constraint from $Z \rightarrow b\bar{b}$, to which they also contribute at one loop [5].

\mathcal{O}_{tt} . It induces (through one loop) a purely right-handed NP effect to the $\gamma t\bar{t}$ and $Z t\bar{t}$ couplings. There exists no Z-peak constraint on \mathcal{O}_{tt} . The observability limit mainly comes from H_{FB} . No effect is generated in top quark decay.

\mathcal{O}_{tb} . Its effect is similar to the \mathcal{O}_{tt} one. However, it also gives a purely right-handed contribution to $Z \rightarrow b\bar{b}$, which is thus providing a LEP 1 constraint. Its observability limit in Table II is just allowed by the present LEP 1 results. No effect is generated in top quark decay.

$\mathcal{O}_{tb}^{(8)}$. This operator produces no effect in the processes studied here or in Z-peak physics.

\mathcal{O}_{qq} and $\mathcal{O}_{qq}^{(8)}$. They contribute (at the one-loop level) to the $t \rightarrow bW$ decay couplings d_j^W giving a $\sigma_{\mu\nu}$ -type contribution affecting only the right-handed b_R field. They also give a $\sigma_{\mu\nu}$ contribution to $Z \rightarrow b\bar{b}$. Both effects are too small to be observable for reasonable values of the coupling constants. They give no contribution to the $\gamma t\bar{t}$ or $Z t\bar{t}$ vertices.

B. Two-quark operators

\mathcal{O}_{t1} . No effect is generated in top quark production or decay or in Z-peak physics.

\mathcal{O}_{t2} . It gives a purely right-handed tree-level contribution to the $Z t\bar{t}$ coupling. At the one-loop level, it also contributes to ϵ_1 and to the $Z b\bar{b}$ vertex in a purely left-handed way. Present constraints from ϵ_1 are marginal. There is no effect on the $\gamma t\bar{t}$ and tbW vertices at the tree level.

\mathcal{O}_{t3} . At the tree level, it produces a right-handed contribution to the tbW vertex. Its most important constraint

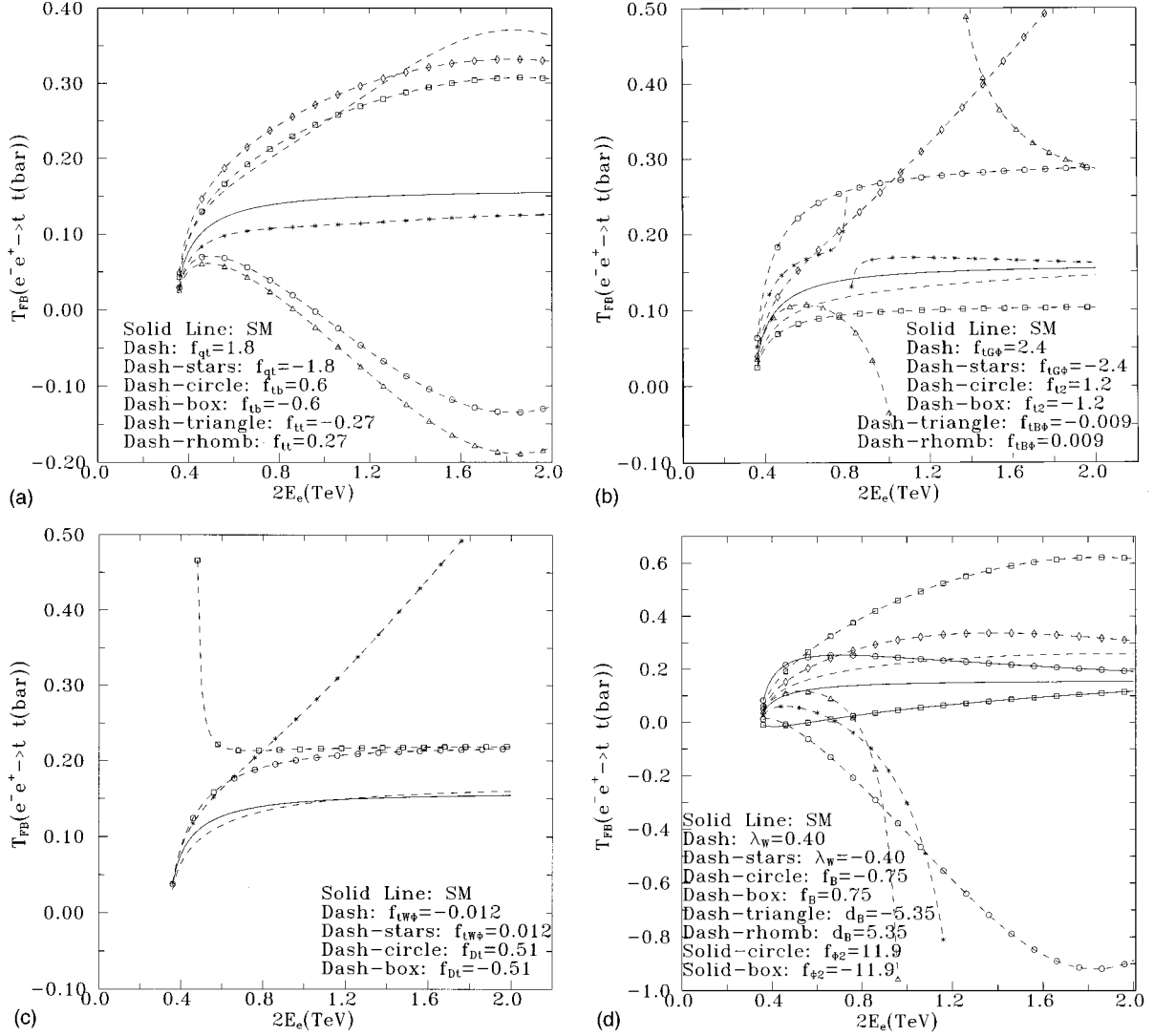


FIG. 5. NP effects on the unpolarized forward-backward asymmetry in the top quark transverse polarization $T_{FB}(e^-e^+ \rightarrow t\bar{t})$, as a function of the c.m. energy $2E_e$, for the NP couplings in Table I. (a) Four-quark NP operators. (b), (c) Two-quark NP operators. (d) Purely bosonic operators; $\mathcal{O}_{W\Phi}$ behaves similarly to \mathcal{O}_W and \mathcal{O}_{UW} gives a very small effect for $d = -5.94$, while for $d = 5.94$ the effect is similar to the one from $\mathcal{O}_{\Phi 2}$ for $f_{\Phi 2} = 11.9$.

should come from $\Gamma(t \rightarrow bW)$. There exists no constraint from Z -peak physics.

\mathcal{O}_{Dt} . At the tree level, it contributes a derivative coupling to the $Zt\bar{t}$ vertex, and has a right-handed contribution to tbW . At the one-loop level, it contributes to ϵ_1 and to $Zb\bar{b}$ in a left-handed way [5]. Present constraints from Z -peak physics are rather marginal. In the linear colliders, the dominant effect should come from $A_{FB, \text{pol}}(e^-e^+ \rightarrow t\bar{t})$. Finally we also note that the two values of the NP scales appearing in Table II correspond to positive and negative f_{Dt} values, respectively.

$\mathcal{O}_{tW\Phi}$. It produces genuine tree-level magnetic-type $\sigma_{\mu\nu}$ couplings to the $\gamma t\bar{t}$, $Zt\bar{t}$, and tbW vertices. The tbW vertex has the additional characteristic that it only involves the left-handed b_L field. $\mathcal{O}_{tW\Phi}$ is presently constrained only by its one-loop contribution to ϵ_3 [5]. The observability limit in the linear colliders arises from the integrated production cross section, the top-quark-decay width, and the decay asymmetries (mainly the D_{FB}^2). This observability limit will supply

only a very minor improvement to the present one from ϵ_3 . This operator could further be checked by looking for an enhancement in the decay $t \rightarrow WZb$, with the Z decaying into lepton pairs [24]. It can also contribute to $t \rightarrow WHb$, provided H is sufficiently light.

$\mathcal{O}_{tB\Phi}$. It produces similar tree-level effects to the $\gamma t\bar{t}$ and $Zt\bar{t}$ vertices, but no contribution to tbW . The effect in the integrated cross section is similar to the one due to $\mathcal{O}_{tW\Phi}$, but the effect on ϵ_3 is weaker, leaving more chance for observability.

$\mathcal{O}_{tG\Phi}$. At the one-loop level, it produces genuine magnetic-type $\sigma_{\mu\nu}$ couplings to the $\gamma t\bar{t}$, $Zt\bar{t}$, and tbW vertices. The tbW vertex has the additional characteristic that it only involves the left-handed b_L field. These properties are like those for $\mathcal{O}_{tW\Phi}$, but appearing at one loop, rather than at the tree level. As a result, there is now no contribution to ϵ_3 at one loop. Future constraints to $\mathcal{O}_{tG\Phi}$ from linear colliders should arise from studies of the integrated cross section, the decay width, and the top-quark-decay asymmetries.

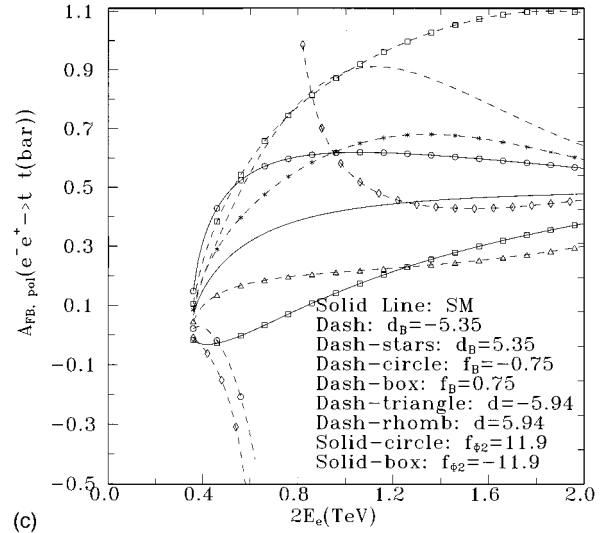
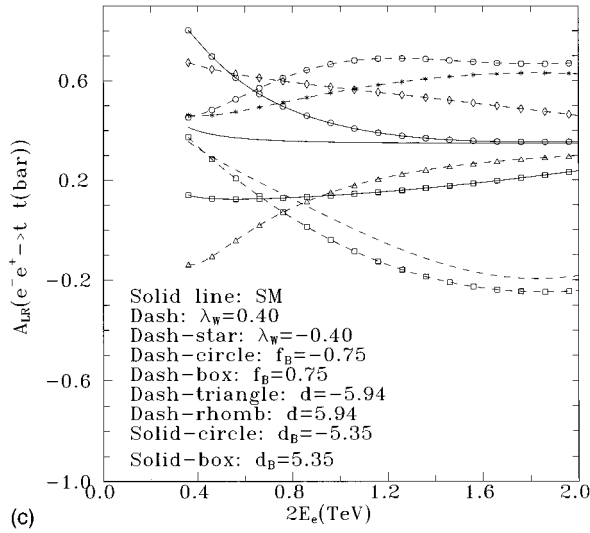
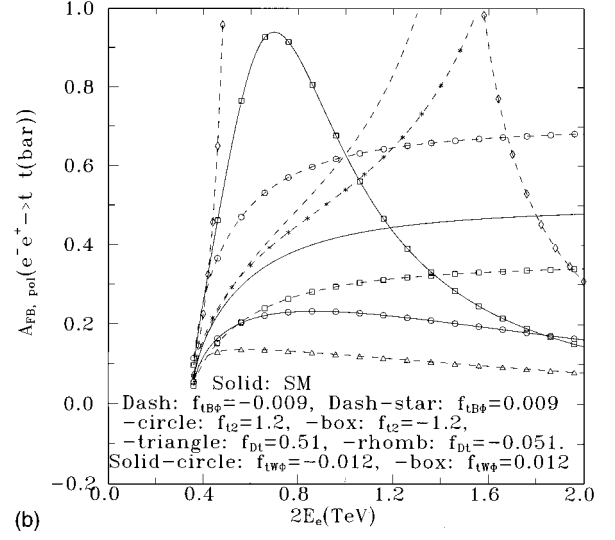
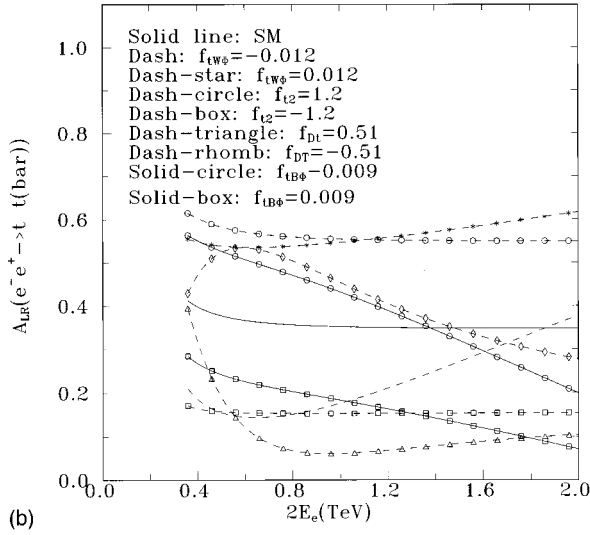
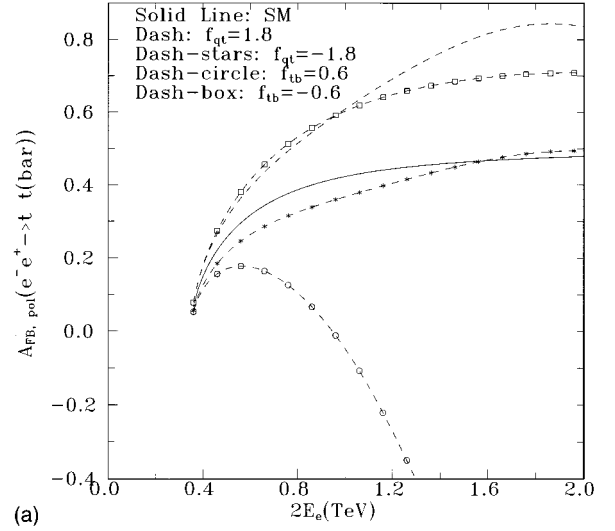
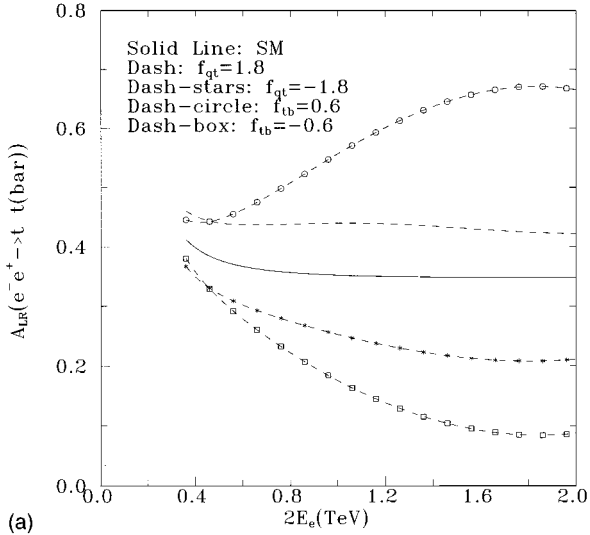
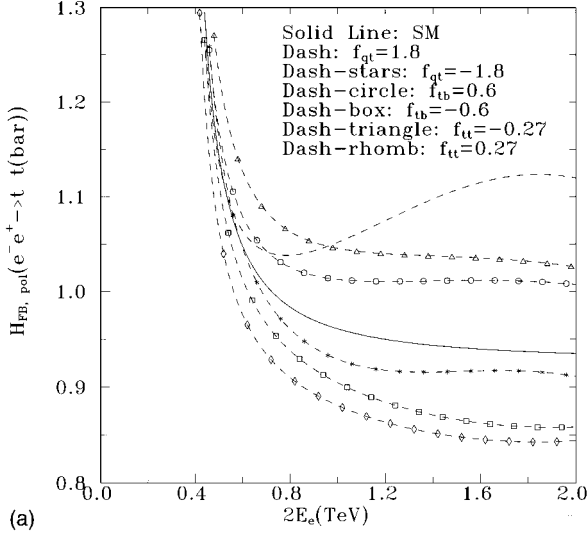
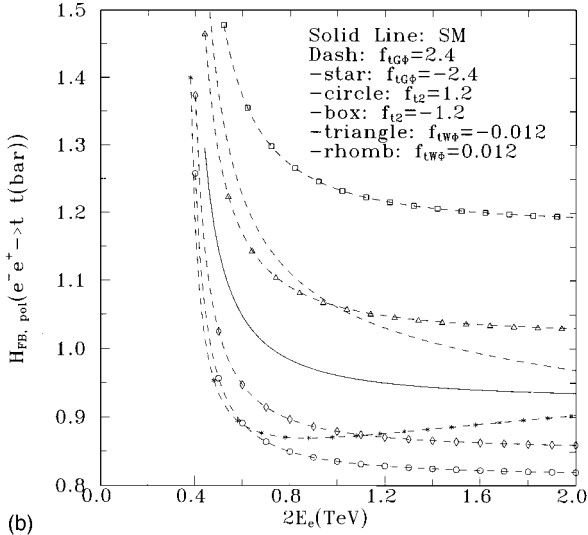


FIG. 6. NP effects, for longitudinally polarized beams, on the left-right asymmetry A_{LR} , for the NP couplings in Table I. (a) Four-quark NP operators; the \mathcal{O}_{tt} effect is similar to \mathcal{O}_{tb} . (b) Two-quark NP operators; the $\mathcal{O}_{tG\Phi}$ effect is very small. (c) Purely bosonic NP operators; the effect of $\mathcal{O}_{W\Phi}$ is of similar magnitude but opposite sign to the one from \mathcal{O}_W , while the \mathcal{O}_{Φ_2} effect is very small.

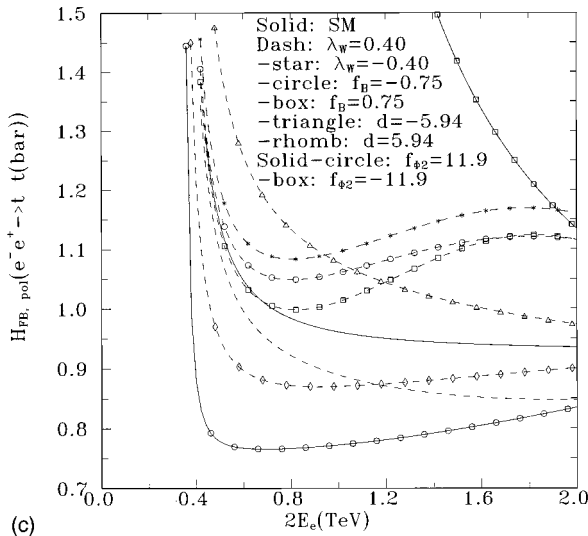
FIG. 7. NP effects on the polarized forward-backward asymmetry in the differential cross section $A_{FB, pol}(e^-e^+ \rightarrow t\bar{t})$, as a function of the c.m. energy $2E_e$, for the NP couplings in Table I. (a) Four-quark NP operators; the \mathcal{O}_{tt} effect is similar to \mathcal{O}_{tb} . (b) Two-quark NP operators; the \mathcal{O}_{t_2} effect is similar to $\mathcal{O}_{tG\Phi}$. (c) Purely bosonic NP operators; $\mathcal{O}_{W\Phi}$ and \mathcal{O}_W effects are of equal magnitude but of opposite sign to the $\mathcal{O}_{B\Phi}$ effect.



(a)

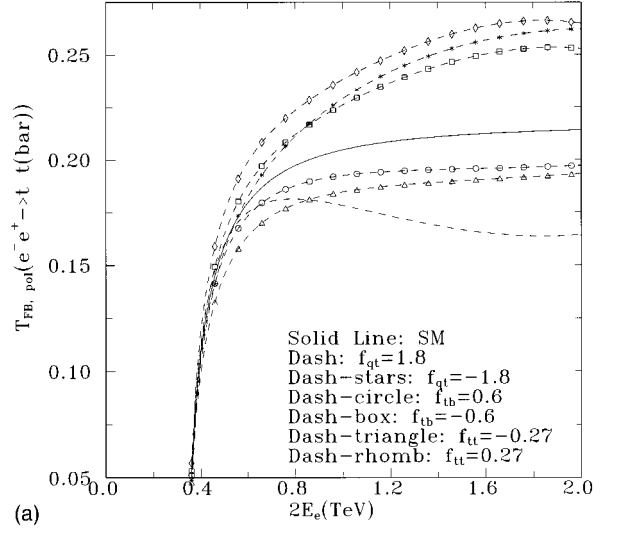


(b)

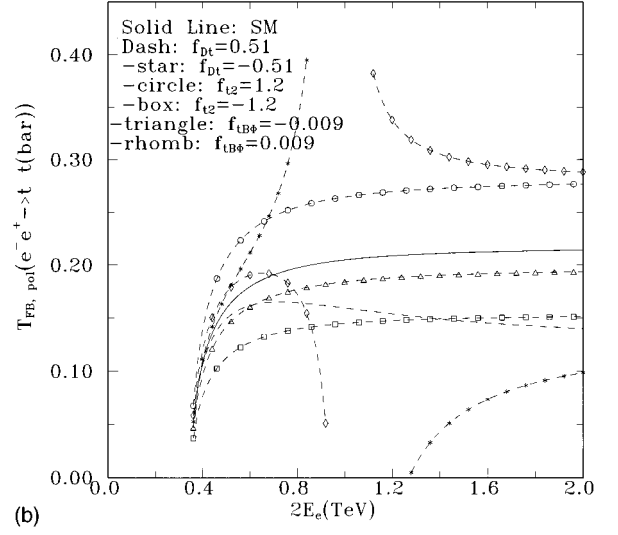


(c)

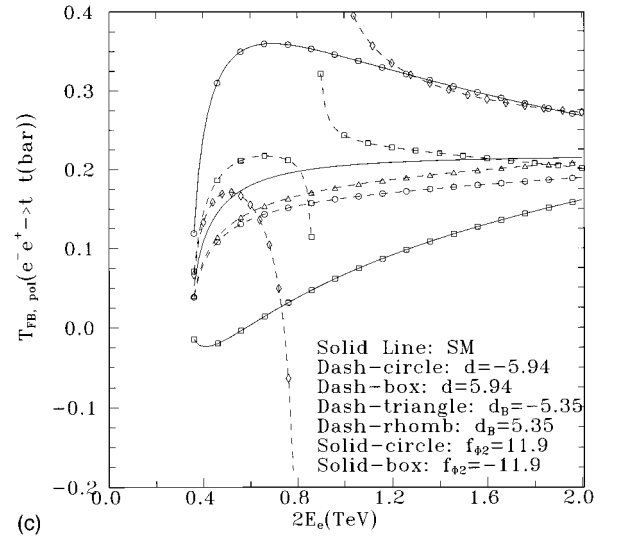
FIG. 8. NP effects on the polarized forward-backward asymmetry in the top quark average helicity $H_{\text{FB, pol}}(e^-e^+ \rightarrow t\bar{t})$, as a function of the c.m. energy $2E_e$, for the NP couplings in Table I. (a) Four-quark NP operators. (b) Two-quark NP operators; $\mathcal{O}_{tB\Phi}$ and $\mathcal{O}_{tW\Phi}$ behave similarly and the \mathcal{O}_{Dt} effect is very small. (c) Purely bosonic operators; \mathcal{O}_{UB} behaves similarly to \mathcal{O}_{UW} and the $\mathcal{O}_{W\Phi}$ effect is similar to \mathcal{O}_W .



(a)



(b)



(c)

FIG. 9. NP effects on the polarized forward-backward asymmetry in the top quark transverse polarization $T_{\text{FB, pol}}(e^-e^+ \rightarrow t\bar{t})$, as a function of the c.m. energy $2E_e$, for the NP couplings in Table I. (a) Four-quark NP operators. (b) Two-quark NP operators; the size of the $\mathcal{O}_{tG\Phi}$ effect $\sim (\frac{1}{2} - \frac{1}{3})\mathcal{O}_{t2}$, while the effect from $\mathcal{O}_{tW\Phi}$ is a rough average of the $\mathcal{O}_{tB\Phi}$ and \mathcal{O}_{Dt} ones. (c) Purely bosonic operators; the effects of \mathcal{O}_W , $\mathcal{O}_{W\Phi}$, and $\mathcal{O}_{B\Phi}$ are not shown since they are small.

TABLE II. Sensitivity limits to “top” and “bosonic” operators in terms of NP couplings and related NP scales Λ_{NP} (TeV).

Operator	$\sqrt{s}=0.5$ TeV	$\sqrt{s}=1$ TeV	$\sqrt{s}=2$ TeV	Other constraints from		
	(Λ_{NP})	(Λ_{NP})	(Λ_{NP})	ϵ_i	$Z \rightarrow b\bar{b}$	LEP 2
\mathcal{O}_{qt}	0.35(1.2)	0.3(1.3)	0.2(1.6)		-0.3 ± 0.2	
$\mathcal{O}_{qt}^{(8)}$	0.07(1.3)	0.06(1.4)	0.04(1.8)		-0.05 ± 0.03	
\mathcal{O}_{tt}	0.02(5.4)	0.015(6.2)	0.01(7.6)			
\mathcal{O}_{tb}	0.07(3.3)	0.04(4.4)	0.03(5.1)		-0.3 ± 0.2	
$\mathcal{O}_{tb}^{(8)}$						
\mathcal{O}_{qq}					38 ± 22	
$\mathcal{O}_{qq}^{(8)}$					8 ± 5	
\mathcal{O}_{i1}						
\mathcal{O}_{i2}	0.011(11)	0.016(9.1)	0.017(8.9)	0.01	0.3 ± 0.2	
\mathcal{O}_{i3}		from decay 0.045 (6.5)				
\mathcal{O}_{Dt}	0.036(3.0, 2.3)	0.03(3.3, 2.6)	0.025(3.6, 2.8)	0.03	-0.12 ± 0.06	
$\mathcal{O}_{tW\Phi}$	0.002(30.5)	0.002(30.5)	0.0015(35)	0.014		
$\mathcal{O}_{tB\Phi}$	0.0015(35)	0.0015(35)	0.0013(38)	0.013		
$\mathcal{O}_{tG\Phi}$	0.02(10)	0.03(6.9)	0.075(2.8)			
\mathcal{O}_W	0.05(1.6)	0.04(1.7)	0.02(2.5)			0.1
$\mathcal{O}_{W\Phi}$	0.08(1.6)	0.06(1.8)	0.04(2.2)			0.1
$\mathcal{O}_{B\Phi}$	0.025(5.0)	0.02(5.6)	0.01(7.9)			0.1
\mathcal{O}_{UW}	0.5(~ 1)	0.8(~ 1)	1.6(~ 1)			0.015
\mathcal{O}_{UB}	0.5(~ 1)	0.6(~ 1)	1.2(~ 1)			0.05
$\mathcal{O}_{\Phi 2}$	0.5	1.0	2.4			0.01

C. Bosonic operators

The effects of these operators on the $\gamma t\bar{t}$, $Zt\bar{t}$, or tbW vertices arise only at the one-loop level.

\mathcal{O}_W . It contributes only to the left-handed $\gamma t\bar{t}$ and $Zt\bar{t}$ form factors. A visible effect from them at a linear collider could appear in H_{FB} and in the cross section. The needed value of the coupling falls just below the visibility domain of LEP 2. No effect is generated in the decay.

$\mathcal{O}_{W\Phi}$. It contributes to the vector and axial vector form factors for the $\gamma t\bar{t}$ and $Zt\bar{t}$ vertices. For the tbW vertex, $\mathcal{O}_{W\Phi}$ creates a left-handed and a derivative coupling, such that a left-handed b_L field is only involved. The visible effects from these couplings at a linear collider are similar to those expected from \mathcal{O}_W , and the same situation with respect to LEP 2 is valid. The expected effects on $t \rightarrow bW$ seem to be below the observability level.

$\mathcal{O}_{B\Phi}$. It induces the same type of couplings as $\mathcal{O}_{W\Phi}$. The sensitivity in H_{FB} is now somewhat better though, so that there exists the possibility of a visible effect from the $\gamma t\bar{t}$ and $Zt\bar{t}$ vertices, which will not be already excluded by LEP 2. The effects on the $t \rightarrow bW$ decay are still unobservable.

\mathcal{O}_{UW} . As in the $\mathcal{O}_{tG\Phi}$ case, it produces genuine magnetic-type $\sigma_{\mu\nu}$ -type couplings to the $\gamma t\bar{t}$, $Zt\bar{t}$, and tbW vertices. The tbW vertex has the additional characteristic that it only involves a left-handed b_L field. Note that these same properties also arise in the $\mathcal{O}_{tW\Phi}$ case, where they are induced at the tree level though. Another thing to note is that \mathcal{O}_{UW} is very mildly constrained by Z-peak physics, which is also valid for $\mathcal{O}_{tG\Phi}$, but not true for $\mathcal{O}_{tW\Phi}$. A most distinctive signature discriminating \mathcal{O}_{UW} from the other two operators may be obtained by studying $e^-e^+ \rightarrow ZH, \gamma H$ [12].

\mathcal{O}_{UB} . As far as the $\gamma t\bar{t}$ and $Zt\bar{t}$ vertices are concerned, the results are similar to the \mathcal{O}_{UW} ones, but their ratio is different. For \mathcal{O}_{UB} we have $d_j^Z/d_j^\gamma = -2s_W^2$, while in the \mathcal{O}_{UW} case we have instead $d_j^Z/d_j^\gamma = -2c_W^2$. No effect appears in the $t \rightarrow bW$ decay.

$\mathcal{O}_{\Phi 2}$. This operator produces a purely axial $Zt\bar{t}$ vertex and a left-handed tbW one. There is no $\gamma t\bar{t}$ vertex induced. Visible effects from $Zt\bar{t}$ could be obtained by looking at H_{FB} and the integrated cross section. The study of $\Gamma(t \rightarrow bW)$ should also help. Like the two previous operators, it could, however, be more strongly constrained by direct Higgs boson production. We also note that the $f_{\Phi 2}$ couplings appearing in Table II are consistent with unitarity only if they are positive. As mentioned above, no constrain on the NP physics is implied in this case [12].

VII. PANORAMA OF RESIDUAL NP EFFECTS IN THE HEAVY QUARK AND BOSONIC SECTORS

We have considered the possibility of anomalous top quark couplings induced by residual NP effects, described by 20 dim=6 gauge-invariant operators. Fourteen of them involve the top quark, and the other six are purely bosonic. The couplings of these operators are associated with a NP scale through unitarity relations.

We have computed the effects of these operators in $e^+e^- \rightarrow t\bar{t}$ and $t \rightarrow bW$ decay. For $e^+e^- \rightarrow t\bar{t}$, these effects are described in terms of six independent form factors for the general $\gamma t\bar{t}$ and $Zt\bar{t}$ vertices. Correspondingly, the $t \rightarrow bW$ decay is described in terms of four couplings denoted as d_j^W . The top quark density matrix can thus be expressed in terms of these form factors and couplings. We have shown

how one can analyze this density matrix in order to get information on the possible forms of NP induced by the various operators. The extra information brought by polarized e^\pm beams is also considered.

Thus, in addition to the integrated unpolarized cross section and the L - R asymmetry, it is possible for polarized beams to construct six different forward-backward asymmetries which should allow one to disentangle the effects of the six form factors d_j^γ , d_j^Z . It is more difficult to disentangle the NP effects on the $t \rightarrow bW$ decay, as no accurate measurement of $\Gamma(t \rightarrow bW)$ is expected, and only one particular combination of decay couplings can easily be measured through an asymmetry with respect to the final lepton, in a semileptonic top quark decay.⁸

The consequences of the NP operators on the above form factors and d_j^W couplings were calculated to first order in the NP couplings. The calculation was done at the tree level, whenever this gave a nonvanishing contribution. In case there was no such contribution, we performed a calculation at the one-loop level, keeping only the leading-logarithmic m_t -enhanced part. Numerical illustrations have been given for the various observables, which reflect the specific properties of each operator. We have then established the corresponding observability limits for each operator in terms of the associated coupling constant and identified the related NP scale. The results can be summarized as follows.

A. Four-quark operators

Among the seven four-quark operators, four of them \mathcal{O}_{qt} , $\mathcal{O}_{qt}^{(8)}$, \mathcal{O}_{tt} , and \mathcal{O}_{tb} , could give sizable one-loop effects in $e^+e^- \rightarrow t\bar{t}$. \mathcal{O}_{tt} is not constrained by Z -peak physics, which means that $e^+e^- \rightarrow t\bar{t}$ would provide a completely new test. The three other operators produce one-loop effects also in $Z \rightarrow b\bar{b}$, which have been studied in [5]. The departure from the SM presently observed in $\Gamma(Z \rightarrow b\bar{b})$, if attributed to one of these three operators, could produce effects which should be easily visible in the \mathcal{O}_{tb} case, but would only be marginally observable for \mathcal{O}_{qt} and $\mathcal{O}_{qt}^{(8)}$.

Concerning the remaining three four-quark operators, we note that \mathcal{O}_{qq} and $\mathcal{O}_{qq}^{(8)}$ are constrained essentially only by $t \rightarrow bW$ [5], while $\mathcal{O}_{tb}^{(8)}$ is not sensitive to Z -peak physics or $e^-e^+ \rightarrow t\bar{t}$, $t \rightarrow bW$.

B. Two-quark operators

Four of the seven two-quark operators, \mathcal{O}_{t2} , \mathcal{O}_{Dt} , $\mathcal{O}_{tW\Phi}$, and $\mathcal{O}_{tB\Phi}$, produce tree-level effects in $e^+e^- \rightarrow t\bar{t}$, while \mathcal{O}_{t3} produces a tree-level effect only in $t \rightarrow bW$. $\mathcal{O}_{tG\Phi}$ contributes at the one-loop level to both production and decay. However, the above four operators \mathcal{O}_{t2} , \mathcal{O}_{Dt} , $\mathcal{O}_{tW\Phi}$, and $\mathcal{O}_{tB\Phi}$ generate also some ϵ_j contribution to Z -peak physics. This seems to already exclude an observable effect from \mathcal{O}_{t2} and \mathcal{O}_{Dt} , but leaves some range for observability to $\mathcal{O}_{tW\Phi}$ and $\mathcal{O}_{tB\Phi}$.

Concerning the rest of the two-quark operators, we remark that \mathcal{O}_{t3} and $\mathcal{O}_{tG\Phi}$ are presently unconstrained; so $e^-e^+ \rightarrow t\bar{t}$ and $t \rightarrow bW \rightarrow bl^+\nu$ would provided genuine new

tests of them. \mathcal{O}_{t1} is not observable through these processes though, and its study requires $t\bar{t}H$ production [28].

C. Bosonic operators

All six bosonic operators contribute at one loop to $e^+e^- \rightarrow t\bar{t}$. Moreover, $\mathcal{O}_{W\Phi}$, \mathcal{O}_{UW} , and $\mathcal{O}_{\Phi 2}$ could also significantly contribute to $t \rightarrow bW$. The operators \mathcal{O}_W , $\mathcal{O}_{W\Phi}$, and $\mathcal{O}_{B\Phi}$ should have an observability level which would not be excluded by LEP 2. Notice that $\mathcal{O}_{W\Phi}$ has a one-loop effect in $Z \rightarrow b\bar{b}$ which could explain the observed anomaly there [4]. In this case large effects should be observed in $t\bar{t}$ production. However, a direct study of these operators in $e^+e^- \rightarrow W^+W^-$ at NLC should be even more stringent.

The three other bosonic operators involving a Higgs field are almost unconstrained at present. So nothing excludes their appearance. However, if the Higgs boson mass is low enough to allow for $e^+e^- \rightarrow HZ$ or $e^+e^- \rightarrow H\gamma$ at LEP 2 and/or at NLC, then these processes would improve the sensitivity limits on these operators by two orders of magnitude.

In conclusion the process $e^+e^- \rightarrow t\bar{t}$ should bring essential information on residual NP effects affecting the heavy quark sector as well as the bosonic (gauge and scalar) sector. Its main interest is that it provides direct tests of the presence of genuine operators involving the third family of quarks. It could give hints about the origin of the anomalies recently observed in the $Zb\bar{b}$ couplings.

ACKNOWLEDGMENTS

We thank Claudio Verzegnassi for having drawn our attention to the m_t^2 -enhanced SM contributions and to the bosonic NP contributions to the $t\bar{t}$ production process. This work was partially supported by EC Contract No. CHRX-CT94-0579 and by the Ministry of Education, Science and Culture, Japan, under a Grant-in-Aid for International Scientific Research Program (No. 07044097).

APPENDIX A: NEW PHYSICS VERTICES GENERATED BY THE EFFECTIVE LAGRANGIAN

It is easy to see that the leading-logarithmic m_t^2 -enhanced NP contributions to $e^-e^+ \rightarrow t\bar{t}$ (up to one-loop order) come exclusively from vertex diagrams for the $\gamma \rightarrow t\bar{t}$ and $Z \rightarrow t\bar{t}$ vertices and from self-energies. The same is of course true for the diagrams affecting $t \rightarrow bW$. Thus, box diagrams never appear. Below we enumerate these contributions for the various operators.

1. Four-quark operators

They contribute to the vertices $\gamma t\bar{t}$, $Z t\bar{t}$, $t bW$ through one-loop diagrams involving a four-quark interaction. This interaction can be read off the following extended expressions. Thus,

$$\mathcal{O}_{qt} = (\bar{t}_L t_R)(\bar{t}_R t_L) + (\bar{b}_L t_R)(\bar{t}_R b_L) \quad (\text{A1})$$

contributes through t and b loops to the $\gamma t\bar{t}$ and $Z t\bar{t}$ vertices, but not to the $t bW$ one;

$$\mathcal{O}_{qt}^{(8)} = (\bar{t}_L \vec{\lambda} t_R) \cdot (\bar{t}_R \vec{\lambda} t_L) + (\bar{b}_L \vec{\lambda} t_R) \cdot (\bar{t}_R \vec{\lambda} b_L) \quad (\text{A2})$$

⁸The same is also true if a hadronic mode is considered.

contributes through a b loop only to the $\gamma t\bar{t}$ and $Zt\bar{t}$ vertices, but not to the tbW one;

$$\mathcal{O}_{tt} = \frac{1}{2}(\bar{t}_R \gamma_\mu t_R)(\bar{t}_R \gamma^\mu t_R) \quad (\text{A3})$$

gives no contribution;

contributes through a t loop to $\gamma t\bar{t}$ and $Zt\bar{t}$, but not to tbW ;

$$\mathcal{O}_{tb} = (\bar{t}_R \gamma_\mu t_R)(\bar{b}_R \gamma^\mu b_R) \quad (\text{A4})$$

contributes through a b loop to $\gamma t\bar{t}$ and $Zt\bar{t}$, but not to $t \rightarrow bW$;

$$\begin{aligned} \mathcal{O}_{qq} = & (\bar{t}_R t_L)(\bar{b}_R b_L) + (\bar{t}_L t_R)(\bar{b}_L b_R) - (\bar{t}_R b_L)(\bar{b}_R t_L) \\ & - (\bar{b}_L t_R)(\bar{t}_L b_R) \end{aligned} \quad (\text{A6})$$

contributes to the tbW vertex, but not to $\gamma t\bar{t}$ and $Zt\bar{t}$; and finally, the

$$\mathcal{O}_{qq}^{(8)} = (\bar{t}_R \vec{\lambda} t_L) \cdot (\bar{b}_R \vec{\lambda} b_L) + (\bar{t}_L \vec{\lambda} t_R) \cdot (\bar{b}_L \vec{\lambda} b_R) - (\bar{t}_R \vec{\lambda} b_L) \cdot (\bar{b}_R \vec{\lambda} t_L) - (\bar{b}_L \vec{\lambda} t_R) \cdot (\bar{t}_L \vec{\lambda} b_R) \quad (\text{A7})$$

contributions are obtained from the \mathcal{O}_{qq} ones, by multiplying by the factor $\frac{16}{3}$.

2. Two-quark operators

Some of the operators in this class contribute already at the tree level, while others only at the one-loop level. The later contributions arise from triangle diagrams for the $\gamma t\bar{t}$, $Zt\bar{t}$, and tbW vertices, as well as from fermion self-energy ones. When an operator contributes at the tree level, we do not care about its one-loop contributions.

For the operator \mathcal{O}_{t1} (after subtracting irrelevant contributions to the top quark mass), we get

$$\mathcal{O}_{t1} = [\chi^+ \chi^- + vH + \frac{1}{2}(\chi^3 \chi^3 + H^2)] \left[\frac{v+H}{\sqrt{2}}(t\bar{t}) + \frac{i}{\sqrt{2}}\chi^3(\bar{t}\gamma^5 t) + i\chi^-(\bar{b}_L t_R) - i\chi^+(\bar{t}_R b_L) \right], \quad (\text{A8})$$

which gives no contribution to the amplitudes we are interested in. For the $\gamma, Z \rightarrow t\bar{t}$ amplitudes, this comes about from the cancellation of the contributions from the vertex triangles involving $(t\bar{t}H)$ and $(tH\chi^3)$ exchanges and the (tH) self-energy, while for the $t \rightarrow bW$ decay, the sum of the $(tH\chi^+)$ triangle and the (tH) self-energy vanishes. The operator

$$\begin{aligned} \mathcal{O}_{t2} = & i(\bar{t}_L \gamma^\mu t_R) \left\{ (\chi^- \partial_\mu \chi^+ - \partial_\mu \chi^- \chi^+) + g(v+H)(\chi^- W_\mu^+ - \chi^+ W_\mu^-) - ig\chi^3(\chi^- W_\mu^+ + \chi^+ W_\mu^-) + ig_Z(1-2s_W^2)Z_\mu \chi^+ \chi^- \right. \\ & \left. + 2ieA_\mu \chi^+ \chi^- - i\frac{g_Z}{2}Z_\mu [(v+H)^2 + \chi^3 \chi^3] + i\chi^3 \partial_\mu H - i(v+H)\partial_\mu \chi^3 \right\} \end{aligned} \quad (\text{A9})$$

contributes at the tree level to $t\bar{t}$ production;

$$\begin{aligned} \mathcal{O}_{t3} = & i(\bar{t}_R \gamma^\mu b_R) \left\{ \frac{i}{\sqrt{2}}[(v+H-i\chi^3)\partial_\mu \chi^+ - \chi^+ \partial_\mu (H-i\chi^3)] + \frac{ig}{\sqrt{2}}\chi^+ W_\mu^- \chi^+ + \frac{ig}{2\sqrt{2}}W_\mu^+(v+H-i\chi^3)^2 \right. \\ & \left. - \frac{g_Z c_W^2}{\sqrt{2}}(v+H-i\chi^3)Z_\mu \chi^+ - \frac{e}{\sqrt{2}}(v+H-i\chi^3)A_\mu \chi^+ \right\} - i(\bar{b}_R \gamma^\mu t_R) \left\{ \frac{-i}{\sqrt{2}}[(v+H+i\chi^3)\partial_\mu \chi^- - \chi^- \partial_\mu (H+i\chi^3)] \right. \\ & \left. - \frac{ig}{\sqrt{2}}\chi^- W_\mu^+ \chi^- - \frac{ig}{2\sqrt{2}}W_\mu^-(v+H+i\chi^3)^2 - \frac{g_Z c_W^2}{\sqrt{2}}(v+H+i\chi^3)Z_\mu \chi^- - \frac{e}{\sqrt{2}}(v+H+i\chi^3)A_\mu \chi^- \right\} \end{aligned} \quad (\text{A10})$$

has no effect on $t\bar{t}$ production, but contributes at the tree level to the $t \rightarrow bW$ decay;

$$\begin{aligned}
\mathcal{O}_{Dl} = & \bar{t}_L \left[\partial_\mu + ig' \frac{2}{3} (-s_W Z_\mu + c_W A_\mu) + i \frac{g_s \vec{\lambda}}{2} \cdot \vec{G}_\mu \right] t_R \left[\frac{1}{\sqrt{2}} \partial_\mu (H + i\chi^3) + \frac{ig}{2\sqrt{2}c_W} (v + H + i\chi^3) Z_\mu - \frac{g}{\sqrt{2}} W_\mu^+ \chi^- \right] \\
& + \bar{b}_L \left[\partial_\mu + ig' \frac{2}{3} (-s_W Z_\mu + c_W A_\mu) + i \frac{g_s \vec{\lambda}}{2} \cdot \vec{G}_\mu \right] t_R \left[i \partial_\mu \chi^- + \frac{g(1-2s_W^2)}{2c_W} Z_\mu \chi^- + e A_\mu \chi^- + \frac{ig}{\sqrt{2}} W_\mu^- \frac{v + H + i\chi^3}{\sqrt{2}} \right] \\
& + \bar{t}_R \left[\tilde{\partial}_\mu - ig' \frac{2}{3} (-s_W Z_\mu + c_W A_\mu) - i \frac{g_s \vec{\lambda}}{2} \cdot \vec{G}_\mu \right] t_L \left[\frac{1}{\sqrt{2}} \partial_\mu (H - i\chi^3) - \frac{ig}{2\sqrt{2}c_W} (v + H - i\chi^3) Z_\mu - \frac{g}{\sqrt{2}} W_\mu^- \chi^+ \right] \\
& + \bar{t}_R \left[\tilde{\partial}_\mu - ig' \frac{2}{3} (-s_W Z_\mu + c_W A_\mu) - i \frac{g_s \vec{\lambda}}{2} \cdot \vec{G}_\mu \right] b_L \left[-i \partial_\mu \chi^+ + \frac{g(1-2s_W^2)}{2c_W} Z_\mu \chi^+ + e A_\mu \chi^+ - \frac{ig}{\sqrt{2}} W_\mu^+ \frac{v + H - i\chi^3}{\sqrt{2}} \right]
\end{aligned} \tag{A11}$$

contributes at the tree level to both production and decay; the same is true for

$$\begin{aligned}
\mathcal{O}_{tW\Phi} = & (c_W Z_{\mu\nu} + s_W A_{\mu\nu}) \left\{ \frac{1}{\sqrt{2}} (\bar{t} \sigma^{\mu\nu} t) (v + H) + \frac{i}{\sqrt{2}} (\bar{t} \sigma^{\mu\nu} \gamma^5 t) \chi^3 - i (\bar{b}_L \sigma^{\mu\nu} t_R) \chi^- + i (\bar{t}_R \sigma^{\mu\nu} b_L) \right\} \chi^+ + i \sqrt{2} (\bar{t}_L \sigma^{\mu\nu} t_R) W_{\mu\nu}^+ \chi^- \\
& - i \sqrt{2} (\bar{t}_R \sigma^{\mu\nu} t_L) W_{\mu\nu}^- \chi^+ + (\bar{b}_L \sigma^{\mu\nu} t_R) W_{\mu\nu}^- (v + H + i\chi^3) + (\bar{t}_R \sigma^{\mu\nu} b_L) W_{\mu\nu}^+ (v + H - i\chi^3),
\end{aligned} \tag{A12}$$

while

$$\begin{aligned}
\mathcal{O}_{tB\Phi} = & (-s_W Z_{\mu\nu} + c_W A_{\mu\nu}) \left\{ \frac{1}{\sqrt{2}} (\bar{t} \sigma^{\mu\nu} t) (v + H) \right. \\
& + \frac{i}{\sqrt{2}} (\bar{t} \sigma^{\mu\nu} \gamma^5 t) \chi^3 + i (b_L \sigma^{\mu\nu} t_R) \chi^- \\
& \left. - i (\bar{t}_R \sigma^{\mu\nu} b_L) \chi^+ \right\}
\end{aligned} \tag{A13}$$

contributes at the tree level only to $t\bar{t}$ production; and finally,

$$\begin{aligned}
\mathcal{O}_{tG\Phi} = & G_{\mu\nu}^a \left\{ \frac{1}{\sqrt{2}} (\bar{t} \sigma^{\mu\nu} \lambda^a t) (v + H) + \frac{i}{\sqrt{2}} (\bar{t} \sigma^{\mu\nu} \lambda^a \gamma^5 t) \chi^3 \right. \\
& \left. + i (\bar{b}_L \sigma^{\mu\nu} \lambda^a t_R) \chi^- - i (\bar{t}_R \sigma^{\mu\nu} \lambda^a b_L) \chi^+ \right\}
\end{aligned} \tag{A14}$$

contributes at one loop to production through the (ttg) triangle and the (tg) self-energy; and to $t \rightarrow bW$ decay through the (tbg) triangle and the (tg) self-energy.

3. Bosonic operators

Contributions in this class arise only at the one-loop level, through triangle and self-energies diagrams. Thus, \mathcal{O}_W [see Eq. (17)] contributes to $e^- e^+ \rightarrow t\bar{t}$ production through the

(WWb) triangle,⁹ but gives no contribution to $t \rightarrow bW$, since the sum of the m_t^2 -enhanced parts of the $(tW\gamma)$ and (tWZ) triangles vanishes. The operator $\mathcal{O}_{W\Phi}$ [see Eq. (18)] contributes to production through the $(tH\chi^3)$ and $(\chi^+ \chi^- b)$ triangles and to decay through the $(t\chi^+ \gamma)$, $(t\chi^+ Z)$, $(b\chi^+ \gamma)$, and $(b\chi^+ Z)$ triangles. In a similar way $\mathcal{O}_{B\Phi}$ [see Eq. (19)] contributes to production through the $(tH\chi^3)$ and $(\chi^+ \chi^- b)$ triangles and to decay through the $(t\chi^+ \gamma)$, $(t\chi^+ Z)$, $(b\chi^+ \gamma)$, and $(b\chi^+ Z)$ triangles. The operator \mathcal{O}_{UW} [see Eq. (20)] contributes to production through the $(tH\gamma)$ and (tHZ) triangles and to decay through (tHW) . Correspondingly, \mathcal{O}_{UB} [see Eq. (21)] contributes to production through the $(tH\gamma)$ and (tHZ) triangles (like in the \mathcal{O}_{UW} case), but gives no contribution to $t \rightarrow bW$ decay. Finally $\mathcal{O}_{\Phi 2}$ [see Eq. (22)] induces a renormalization of the physical Higgs field at the tree level. This, in turn, gives contributions to production, through the ttH triangle and the tH self-energy and to decay through the tH self-energy.

APPENDIX B: TOP QUARK DECAY DISTRIBUTIONS

As discussed in Sec. IV, it is convenient to express the three-body phase space $d\Phi_3(bl\nu)$ in terms of the Euler angles determining the t -quark-decay plane. We start from the process $e^-(k)e^+(k') \rightarrow t(p)\bar{t}(p')$ in the center-of-mass frame, where the momenta are indicated in parentheses, and by θ we denote the (e^-, t) scattering angle. The t frame is defined with its z axis along the top quark momentum. The

⁹ \mathcal{O}_W does not produce m_t^2 terms but it must be taken into consideration since the contribution is proportional to s which is larger than $4m_t^2$ for the process under consideration.

x axis is taken in the $(t\bar{t})$ production plane, so that the y axis is perpendicular to it and along the direction of $\vec{k} \times \vec{p}$. In order to describe the decay plane of the process $t \rightarrow b(p_b)l^+(p_l)\nu_l(p_\nu)$, in the t frame (with the momenta indicated in parentheses), we define the Euler rotation

$$R_{\varphi_1 \vartheta_1 \psi_1} = \begin{pmatrix} \cos\varphi_1 & -\sin\varphi_1 & 0 \\ \sin\varphi_1 & \cos\varphi_1 & 0 \\ 0 & 0 & 1 \end{pmatrix} \begin{pmatrix} \cos\vartheta_1 & 0 & \sin\vartheta_1 \\ 0 & 1 & 0 \\ -\sin\vartheta_1 & 0 & \cos\vartheta_1 \end{pmatrix} \\ \times \begin{pmatrix} \cos\psi_1 & -\sin\psi_1 & 0 \\ \sin\psi_1 & \cos\psi_1 & 0 \\ 0 & 0 & 1 \end{pmatrix}, \quad (\text{B1})$$

where $(\varphi_1, \vartheta_1, \psi_1)$ satisfy $0 \leq \varphi_1, \psi_1 < 2\pi, 0 \leq \vartheta_1 \leq \pi$. The meaning of these angles is given by remarking that the normal to the t -quark-decay plane, with its orientation defined by $(\vec{p}_b \times \vec{p}_l)$, is given by

$$\hat{n} = R_{\varphi_1 \vartheta_1 \psi_1} \begin{pmatrix} 0 \\ 0 \\ 0 \end{pmatrix} = \begin{pmatrix} \sin\vartheta_1 \cos\varphi_1 \\ \sin\vartheta_1 \sin\varphi_1 \\ \cos\vartheta_1 \end{pmatrix}. \quad (\text{B2})$$

Thus, ϑ_1, φ_1 determine the \hat{n} orientation, while the b quark momentum in the t rest frame is determined from ψ_1 through the relation

$$\vec{p}_b = |\vec{p}_b| R_{\varphi_1 \vartheta_1 \psi_1} \begin{pmatrix} 1 \\ 0 \\ 0 \end{pmatrix} \\ = |\vec{p}_b| \begin{pmatrix} \cos\varphi_1 \cos\vartheta_1 \cos\psi_1 - \sin\varphi_1 \sin\psi_1 \\ \sin\varphi_1 \cos\vartheta_1 \cos\psi_1 + \cos\varphi_1 \sin\psi_1 \\ -\sin\vartheta_1 \cos\psi_1 \end{pmatrix}. \quad (\text{B3})$$

The corresponding expression for the l^+ momentum is obtained from Eq. (B3) by substituting $\vec{p}_b \rightarrow \vec{p}_l$ and $\psi_1 \rightarrow \psi_1 + y_{12}$, where y_{12} is the angle between the b and l^+ momenta (in the t rest frame). To summarize, it is worthwhile to remark that the above Euler rotation moves the z axis of the t frame along the normal to the t -quark-decay plane, while the x axis is brought along the \vec{p}_b momentum, which of course lies within the decay plane.

Finally θ_l is the angle between the lepton momentum and the top quark momentum in the W rest frame, and it is related to the l^+ energy in the t frame by

$$E_l = |\vec{p}_l| = \frac{m_t^2 + M_W^2 - \cos\theta_l(m_t^2 - M_W^2)}{4m_t}, \quad (\text{B4})$$

where the (b, l^+) masses are neglected. Using these Euler angles, we obtain

$$\delta[(p_t + p_\nu)^2 - M_W^2] d\Phi_3(bl\nu_l) \\ \Rightarrow \frac{(m_t^2 - M_W^2)}{64m_t^2(2\pi)^9} d\varphi_1 d\cos\vartheta_1 d\psi_1 d\cos\theta_l, \quad (\text{B5})$$

for the three-body phase space in the case where the $l\nu$ pair is at the W mass shell [25].

The general expression of the differential cross section for $e^+e^- \rightarrow t\bar{t}$ with $t \rightarrow bW \rightarrow bl\nu_l$ and linearly polarized $[L(R)e^-]$ and $[R(L)e^+]$ beams is written [compare Eqs. (55) and (56)] as

$$\frac{d\sigma^{L,R}}{d\cos\theta d\varphi_1 d\cos\vartheta_1 d\psi_1 d\cos\theta_l} \\ = \left(\frac{3\beta_t}{32(2\pi)^5 s} \right) \frac{G_F^2 M_W^3}{\Gamma_W \Gamma_t m_t} \left(\frac{m_t^2 - M_W^2}{4m_t} \right)^2 \rho_{\tau_1 \tau_2}^{L,R} \mathcal{R}_{\tau_1 \tau_2}, \quad (\text{B6})$$

where $\beta_t = (1 - 4m_t^2/s)^{1/2}$. In Eq. (B6), $\rho^{L,R}$ is the top quark density matrix defined in Eq. (50), while \mathcal{R} is related to the top-quark-decay matrix $t_{\tau_1 \tau_2}$ introduced in Eqs. (56) and (58) by

$$\frac{t_{\tau_1 \tau_2}}{d\varphi_1 d\cos\vartheta_1 d\psi_1 d\cos\theta_l} \\ = \frac{G_F^2 M_W^3}{2(2\pi)^4 \Gamma_W \Gamma_t m_t} \left(\frac{m_t^2 - M_W^2}{4m_t} \right)^2 \mathcal{R}_{\tau_1 \tau_2}. \quad (\text{B7})$$

The ρ matrix depends only on the $e^-e^+ \rightarrow t\bar{t}$ production and the angle θ [see Eq. (50)], while \mathcal{R} depends on the three Euler angles φ_1, ϑ_1 , and ψ_1 [defined in Eq. (B1)] and on the d_j^W couplings of Eq. (51) and the angle θ_l . To simplify the expression for \mathcal{R} , we only keep terms linear in the NP and the one-loop SM contributions to the couplings d_j^W , defining $\bar{d}_j^W \equiv d_j^{W,SM1} + d_j^{W,NP}$. We thus get

$$\rho_{\tau_1 \tau_2}^{L,R} \mathcal{R}_{\tau_1 \tau_2} = \frac{1}{2}(\rho_{++} + \rho_{--})^{L,R} (\mathcal{R}_{++} + \mathcal{R}_{--}) \\ + \frac{1}{2}(\rho_{++} - \rho_{--})^{L,R} (\mathcal{R}_{++} - \mathcal{R}_{--}) \\ + \rho_{+-}^{L,R} (\mathcal{R}_{+-} + \mathcal{R}_{-+}), \quad (\text{B8})$$

where

$$\mathcal{R}_{++} + \mathcal{R}_{--} = (1 + \bar{d}_1^W - \bar{d}_2^W) [M_W^2 V_1 + m_t^2 V_2] + \left(\frac{m_t^2 - M_W^2}{m_t} \right) \\ \times (\bar{d}_3^W + \bar{d}_4^W) m_t^2 V_2, \quad (\text{B9})$$

$$\mathcal{R}_{+-} - \mathcal{R}_{-+} = (1 + \bar{d}_1^W - \bar{d}_2^W) [m_t^2 V_4 - M_W^2 V_3 + 2m_t M_W V_5] \\ + \left(\frac{m_t^2 - M_W^2}{m_t} \right) (\bar{d}_3^W + \bar{d}_4^W) [m_t^2 V_4 + m_t M_W V_5], \quad (\text{B10})$$

$$\begin{aligned} \mathcal{R}_{+-} + \mathcal{R}_{-+} = & (1 + \bar{d}_1^W - \bar{d}_2^W)[M_W^2 V_6 - m_t^2 V_7 - 2m_t M_W V_8] \\ & - \left(\frac{m_t^2 - M_W^2}{m_t} \right) (\bar{d}_3^W + \bar{d}_4^W)[m_t^2 V_7 + m_t M_W V_8], \end{aligned} \quad (\text{B11})$$

and

$$V_1 = (1 + \cos\theta_l)^2, \quad V_2 = \sin^2\theta_l, \quad (\text{B12})$$

$$V_3 = (1 + \cos\theta_l)^2 \sin\vartheta_1 \cos\psi_1, \quad V_4 = \sin^2\theta_l \sin\vartheta_1 \cos\psi_1, \quad (\text{B13})$$

$$V_5 = (1 + \cos\theta_l) \sin\theta_l \sin\vartheta_1 \sin\psi_1, \quad (\text{B14})$$

$$V_6 = (1 + \cos\theta_l)^2 (\cos\varphi_1 \cos\vartheta_1 \cos\psi_1 - \sin\varphi_1 \sin\psi_1), \quad (\text{B15})$$

$$V_7 = \sin^2\theta_l (\cos\varphi_1 \cos\vartheta_1 \cos\psi_1 - \sin\varphi_1 \sin\psi_1), \quad (\text{B16})$$

$$V_8 = \sin\theta_l (1 + \cos\theta_l) (\cos\varphi_1 \cos\vartheta_1 \sin\psi_1 + \sin\varphi_1 \cos\psi_1). \quad (\text{B17})$$

Using the angular dependence in Eqs. (B9)–(B17) and constructing appropriate averages over φ_1 , ϑ_1 , and ψ_1 , it is possible to project quantities proportional to the ρ factors in each of the three terms of the right-hand side (RHS) in Eq. (B8). More explicitly these quantities consist of products of the corresponding ρ elements and of functions of θ_l . Remember that the ρ elements depend only on θ and the NP couplings for $\gamma t\bar{t}$ and $Z t\bar{t}$. Thus, the subsequent construction of forward-backward asymmetries with respect to either θ or θ_l , respectively, allows the isolation of either the ρ factor or of the corresponding combination of the \bar{d}_i^W couplings. To do this we first describe the ρ elements entering the three terms in Eq. (B8). For this, it is convenient to define, for $i=1,2,3$ [compare Eq. (44)]

$$d_i^L = d_i^\gamma + \frac{1 - 2s_W^2}{4s_W^2 c_W^2} \chi d_i^Z, \quad d_i^R = d_i^\gamma - \frac{\chi}{2c_W^2} d_i^Z, \quad (\text{B18})$$

where $\chi \equiv s/(s - M_Z^2)$ and the Z width is neglected for $s = q^2 > 4m_t^2$. We then have

$$\begin{aligned} (\rho_{++} + \rho_{--})^{L,R} = & e^4 \sin^2\theta \left(\frac{8m_t^2}{s} \right) \left[d_1^{L,R} - \frac{2|\vec{p}|^2}{m_t} d_3^{L,R} \right]^2 \\ & + 2e^4 (1 + \cos^2\theta) \left[(d_1^{L,R})^2 + \frac{4|\vec{p}|^2}{s} (d_2^{L,R})^2 \right] \\ & \mp e^4 \cos\theta \left(\frac{16|\vec{p}|^2}{\sqrt{s}} \right) d_1^{L,R} d_2^{L,R}, \end{aligned} \quad (\text{B19})$$

$$\begin{aligned} (\rho_{++} - \rho_{--})^{L,R} = & e^4 (1 + \cos^2\theta) \left(\frac{8|\vec{p}|^2}{\sqrt{s}} \right) d_1^{L,R} d_2^{L,R} \\ & \mp 4e^4 \cos\theta \left[(d_1^{L,R})^2 + \frac{4|\vec{p}|^2}{s} (d_2^{L,R})^2 \right], \end{aligned} \quad (\text{B20})$$

$$\begin{aligned} \rho_{+-}^{L,R} = & e^4 \sin\theta \left(\frac{4m_t}{\sqrt{s}} \right) \left[d_1^{L,R} - \frac{2|\vec{p}|^2}{m_t} d_3^{L,R} \right] \\ & \times \left[\pm d_1^{L,R} - \frac{2|\vec{p}|^2}{\sqrt{s}} \cos\theta d_2^{L,R} \right]. \end{aligned} \quad (\text{B21})$$

For unpolarized e^\mp beams, only the $(L+R)/2$ combination, like, e.g., $d\sigma^{\text{unpol}} = (d\sigma^L + d\sigma^R)/2$ or $(\rho^L + \rho^R)/2$, is measurable through forward-backward asymmetries. There are three ρ and \mathcal{R} elements that can be studied this way. If longitudinal electron beam polarization is available, we can also consider the corresponding three $(\rho^L - \rho^R)$ combinations and their forward-backward asymmetries.

Thus, by integrating both sides of Eq. (B6) over $d\varphi_1 d\cos\vartheta_1 d\psi_1$, the first term on the RHS of Eq. (B8) is projected. Integrating also over $\cos\theta_l$ and constructing the forward-backward asymmetry with respect to the $t\bar{t}$ production angle θ allows the study of the NP effects in $(\rho_{++} + \rho_{--})^{L,R}$. This asymmetry is of course the usual forward-backward asymmetry in the differential cross section for the top quark production through $e^+e^- \rightarrow t\bar{t}$. We thus have

$$A_{\text{FB}} = \frac{(3\beta_l/2)[d_1^R d_2^R - d_1^L d_2^L]}{(d_1^L)^2 + (d_1^R)^2 + \beta_l^2 [(d_2^L)^2 + (d_2^R)^2] + (2m_t^2/s) \{ [d_1^L - (2|\vec{p}|^2/m_t) d_3^L]^2 + [d_1^R - (2|\vec{p}|^2/m_t) d_3^R]^2 \}}, \quad (\text{B22})$$

for the unpolarized case, while for the L - R one we have

$$A_{\text{FB,pol}} = \frac{-(3\beta_l/2)[d_1^R d_2^R + d_1^L d_2^L]}{(d_1^L)^2 - (d_1^R)^2 + \beta_l^2 [(d_2^L)^2 - (d_2^R)^2] + (2m_t^2/s) \{ [d_1^L - (2|\vec{p}|^2/m_t) d_3^L]^2 - [d_1^R - (2|\vec{p}|^2/m_t) d_3^R]^2 \}}. \quad (\text{B23})$$

The preceding method for constructing the forward-backward asymmetry is just given in order to emphasize its similarity to the methods for constructing the other asymmetries below. Consequently, by multiplying both sides of Eq. (B6) by either $\cos\psi_1$ or $\sin\psi_1$ and integrating over $d\varphi_1 d\cos\vartheta_1 d\psi_1$, the second term on the RHS of Eq. (B8) is projected. Integrating then over $\cos\theta_l$, we construct the forward-backward asymmetry with respect to θ for the quantity $(\rho_{++} - \rho_{--})^{L,R}$ controlling the angular distribution of the average helicity of the produced top quark. Thus, in terms of the couplings defined in Eq. (44), the forward-backward asymmetry in the top quark average helicity is

$$H_{\text{FB}} = -\frac{3\{(d_1^L)^2 - (d_1^R)^2 + \beta_t^2[(d_2^L)^2 - (d_2^R)^2]\}}{8\beta_t[d_1^L d_2^L + d_1^R d_2^R]}, \quad (\text{B24})$$

for the e^\pm unpolarized case, while for the L - R one we have

$$H_{\text{FB,pol}} = -\frac{3\{(d_1^L)^2 + (d_1^R)^2 + \beta_t^2[(d_2^L)^2 + (d_2^R)^2]\}}{8\beta_t[d_1^L d_2^L - d_1^R d_2^R]}. \quad (\text{B25})$$

Finally the third term on the RHS of Eq. (B8) is projected by multiplying both sides of Eq. (B6) by quantities like any one of

$$\cos\psi_1 \sin\varphi_1, \quad \sin\psi_1 \cos\varphi_1 \cos\vartheta_1, \quad (\text{B26})$$

$$\sin\psi_1 \sin\varphi_1, \quad \cos\psi_1 \cos\varphi_1 \cos\vartheta_1, \quad (\text{B27})$$

and integrating over $d\varphi_1 d\cos\vartheta_1 d\psi_1$. The subsequent integration over $\cos\theta_l$ allows the construction of the forward-backward asymmetry with respect to θ for the quantity $\rho_{+-}^{L,R}$ controlling the angular distribution of the top quark average transverse polarization. Thus, for unpolarized e^\mp beams, the forward-backward asymmetry in the top quark transverse polarization is obtained, which is given by

$$T_{\text{FB}} = -\frac{4\beta_t[d_1^L d_2^L + d_1^R d_2^R - (2|\vec{p}|^2/m_t)(d_3^L d_2^L + d_3^R d_2^R)]}{3\pi[(d_1^L)^2 - (d_1^R)^2 - (2|\vec{p}|^2/m_t)(d_3^L d_1^L - d_3^R d_1^R)]}, \quad (\text{B28})$$

while for polarized beams the L - R case gives

$$T_{\text{FB,pol}} = \frac{-4\beta_t[d_1^L d_2^L - d_1^R d_2^R - (2|\vec{p}|^2/m_t)(d_3^L d_2^L - d_3^R d_2^R)]}{3\pi[(d_1^L)^2 + (d_1^R)^2 - (2|\vec{p}|^2/m_t)(d_3^L d_1^L + d_3^R d_1^R)]}. \quad (\text{B29})$$

For any of the preceding three types of forward-backward asymmetries sensitive to the $t\bar{t}$ production couplings, we can construct corresponding asymmetries sensitive to the decay couplings d_j^W . This is done in all cases by integrating at the last step over $\cos\theta$ (instead of over $\cos\theta_l$ done above) and constructing the forward-backward asymmetry with respect to θ_l . As before, we always work to linear order in d_j^W . Thus, for the first case which led to Eqs. (B22) and (B23) we get

$$D_{\text{FB}}^1 = \frac{3M_W^2}{2(2M_W^2 + m_t^2)} \left[1 - \frac{m_t(m_t^2 - M_W^2)}{2M_W^2 + m_t^2} (\bar{d}_3^W + \bar{d}_4^W) \right]. \quad (\text{B30})$$

For the second case, we have already stated that the asymmetries (B24) and (B25) are obtained by using either $\cos\psi_1$ or $\sin\psi_1$ to project out the ρ factor in the second term on the RHS of Eq. (B8). For the θ_l asymmetry though, these two projections give different asymmetries. Thus the asymmetry obtained through $\cos\psi_1$ is

$$D_{\text{FB}}^2 = \frac{-3M_W^2}{2(m_t^2 - 2M_W^2)} \left[1 - \frac{m_t(m_t^2 - M_W^2)}{m_t^2 - 2M_W^2} (\bar{d}_3^W + \bar{d}_4^W) \right], \quad (\text{B31})$$

while the one obtained from $\sin\psi_1$ is independent of \bar{d}_j^W and equal to

$$D_{\text{FB}}^3 = \frac{4}{3\pi}. \quad (\text{B32})$$

Finally in the third case, we get D_{FB}^2 for the asymmetry obtained through the projector (B27) and D_{FB}^3 for the asymmetry obtained through Eq. (B26).

To linear order in the NP couplings, all these asymmetries can be expressed as a product of a factor describing the SM contribution and another factor describing the NP correction. For this NP correction a tree-level calculation is sufficient. Any QCD and one-loop radiative corrections should in general be incorporated in the SM factor only. The QCD corrections have to some extent been studied in [22,19] and have been found to be rather small. In any case this is something which we plan to do in the future. It is also interesting to remark that while the production asymmetries are sufficient to determine all d_j^γ and d_j^Z couplings even in the unpolarized case, this is not possible for the decay couplings. To linear order in the NP top-quark-decay couplings, the above asymmetries are only sensitive to the combination $\bar{d}_3^W + d_4^W$.

Finally we should also remark that the case where the t quark decays hadronically, while $\bar{t} \rightarrow \bar{b}l^+ \bar{\nu}$ is very similar. Thus, if the orientation of the \bar{t} rest frame is defined to be like the one obtained from the t frame by rotating it by 180° around the perpendicular to the $t\bar{t}$ production plane, and if the new Euler angles for the \bar{t} -quark-decay plane are called $(\varphi_2, \vartheta_2, \psi_2)$, and θ_l is defined analogously, then all formulas in this appendix remain the same, except Eqs. (B12)–(B17) where we should replace

$$\varphi_1, \psi_1, \vartheta_1 \Rightarrow \varphi_2, \psi_2, -\vartheta_2. \quad (\text{B33})$$

This way, all forward-backward asymmetries remain formally identical. Note, though, that the definition of the top quark production angle θ implies that (forward-backward) for \bar{t} means that we should subtract as

$$\text{backward}(\bar{t}) - \text{forward}(\bar{t}). \quad (\text{B34})$$

- [1] M. Veltman, Nucl. Phys. **B123**, 89 (1977); M.E. Peskin and T. Takeuchi, Phys. Rev. Lett. **65**, 964 (1990); G. Altarelli and R. Barbieri, Phys. Lett. B **253**, 161 (1991).
- [2] A. Akhundov, D. Bardin, and T. Riemann, Nucl. Phys. **B276**, 1 (1986); W. Beenaker and W. Hollik, Z. Phys. C **40**, 141 (1988); B.W. Lynn and R.G. Stuart, Phys. Lett. B **252**, 676 (1990); J. Bernabeu, A. Pich, and A. Santamaria, Nucl. Phys. **B263**, 326 (1991).
- [3] P.B. Renton, in *Proceedings of the 17th International Symposium on Lepton-Photon Interactions*, Beijing, China, 1995, edited by Zheng Zhi Leng and Chen He Sheng (World Scientific, Singapore, 1996), p. 35; K. Hagiwara, *ibid.*, p. 63; P. Langacker, Report No. NSF-ITP-95-140, UPR-0683T, 1995 (unpublished); D. G. Charlton, in *Proceedings of EPS International Conference on High Energy Physics*, Brussels, Belgium, 1995, edited by J. Lemonne, C. van der Velde, and F. Verbeure (World Scientific, Singapore, 1996), p. 266; P. S. Wells, presented at CERN, 1995 (unpublished).
- [4] F.M. Renard and C. Verzegnassi, Phys. Lett. B **345**, 500 (1995).
- [5] G. Gounaris, F.M. Renard, and C. Verzegnassi, Phys. Rev. D **52**, 451 (1995).
- [6] J.D. Wells, C. Kolda, and G.L. Kane, Phys. Lett. B **338**, 219 (1994); C.T. Hill and X. Zhang, Phys. Rev. D **51**, 3563 (1995); T.G. Rizzo, *ibid.* **51**, 3811 (1995); H. Georgi, L. Kaplan, D. Morin, and A. Schenk, *ibid.* **51**, 3888 (1995); Z. Zhang and B.-L. Young, *ibid.* **51**, 6584 (1995); E. Ma and D. Eng, *ibid.* **53**, 255 (1996); J. Solà, Report No. hep-ph/9508339 (unpublished); E. Ma, Phys. Rev. D **53**, 2276 (1996); P. Bamert *et al.*, *ibid.* **54**, 4275 (1996); D. Atwood *et al.*, *ibid.* **54**, 3296 (1996); P.H. Chankowski and S. Pokorski, Report No. hep-ph/9603310 (unpublished); D. Comelli and J.P. Silva, Phys. Rev. D **54**, 1176 (1996).
- [7] P. Chiappetta, J. Layssac, F.M. Renard, and C. Verzegnassi, Phys. Rev. D **54**, 789 (1996); G. Altarelli *et al.*, Phys. Lett. B **375**, 292 (1996).
- [8] K. Hagiwara *et al.*, Phys. Lett. B **283**, 353 (1992); Phys. Rev. D **48**, 2182 (1993).
- [9] A. De Rújula *et al.*, Nucl. Phys. **B384**, 3 (1992).
- [10] G.J. Gounaris *et al.*, in *e^+e^- Collisions at 500 GeV: The Physics Potential*, Proceedings of the Workshop, Munich, Annecy, Hamburg, edited by P. Zerwas (DESY Report No. 92-123B, Hamburg, 1992), p. 735; M. Bilenky, J.L. Kneur, F.M. Renard, and D. Schildknecht, Nucl. Phys. **B419**, 240 (1994); M. Bilenky, J.L. Kneur, F.M. Renard, and D. Schildknecht, *ibid.* **B409**, 22 (1993).
- [11] G.J. Gounaris *et al.* in ‘‘Physics at LEP2,’’ Yellow Report CERN 96-01, edited by G. Altarelli, T. Sjöstrand, and F. Zwirner (Geneva, 1996).
- [12] G. Gounaris, F.M. Renard, and N.D. Vlachos, Nucl. Phys. **B459**, 51 (1996).
- [13] K. Hagiwara and M.L. Stong, Z. Phys. C **62**, 99 (1994); W. Kilian, M. Krämer, and P.M. Zerwas, Phys. Lett. B **381**, 243 (1996).
- [14] G.J. Gounaris, D. Papadamou, and F.M. Renard, Report No. PM/96-28, THES-TP96/09, hep-ph/9609437 (unpublished), Vol. 1, p. 525.
- [15] G.J. Gounaris, F.M. Renard, and G. Tsirigoti, Phys. Lett. B **338**, 51 (1994); Phys. Lett. B **350**, 212 (1995).
- [16] K. Hagiwara, S. Matsumoto, and R. Szalapski, Phys. Lett. B **357**, 411 (1995).
- [17] A. Blondel, F.M. Renard, L. Trentadue, and C. Verzegnassi, Montpellier Report No. PM/96-14, 1996 (unpublished).
- [18] G.J. Gounaris, J. Layssac, and F.M. Renard, Phys. Lett. B **332**, 146 (1994); G.J. Gounaris, J. Layssac, J.E. Paschalis, and F.M. Renard, Z. Phys. C **66**, 619 (1995).
- [19] B. Lampe, Nucl. Phys. **B454**, 506 (1995); **B458**, 23 (1996).
- [20] G. Altarelli, R. Barbieri, and F. Caravaglios, Phys. Lett. B **314**, 357 (1993); G. Altarelli, *Proceedings of the International Symposium on Radiative Connections*, Gatlinburg, 1994, p. 491, Report No. CERN-TH.7464/94 (unpublished); and Ref. [3].
- [21] D. Chang, W.-Y. Keung, and I. Phillips, Nucl. Phys. **B408**, 286 (1993).
- [22] K.G. Chetykin, A.H. Hoang, J.H. Kühn, M. Steinhauser, and T. Teubner, Report No. hep-ph/9605311 (unpublished).
- [23] D.O. Carlson and C.-P. Yuan, Report No. MSUHEP-50823, 1995 (unpublished); C.-P. Yuan, Report No. hep-ph/9604434 (unpublished).
- [24] A.P. Heinson, presented at the XXXI Rencontres de Moriond, 1996 (unpublished); Report No. hep-ex/9605010 (unpublished).
- [25] Particle Data Group, L. Montanet *et al.*, Phys. Rev. D **50**, 1173 (1995), p. 1290, Eqs. (23.13) and (23.20).
- [26] F.M. Renard and C. Verzegnassi, Phys. Rev. D **52**, 1369 (1995); **53**, 1290 (1996).
- [27] M. Lindner, Z. Phys. C **31**, 295 (1986); G. Altarelli and G. Isidori, Phys. Lett. B **337**, 141 (1994).
- [28] X. Zhang, S.K. Lee, K. Whisnant, and B.-L. Young, Phys. Rev. D **50**, 7042 (1994).